

The Role of Porous Medium Modeling in Biothermofluids

Arunn Narasimhan

Abstract | Biothermology or Bio- fluid flow and heat transfer is an important and developing subdivision of bioengineering. Seeking simplifications for biological processes that are inherently complex, through porous medium models, is an exciting and useful multidisciplinary pursuit. This review presents an overview of the post-2002 research on the modelling aspects of several biothermofluid processes based primarily on the porous medium approach. Beginning with a definition for porous medium suited for analysing transport phenomena, concepts of volume averaging, momentum and energy conservation statements are briefly discussed to motivate the ensuing review discussions. Porous medium modelling of several biomedical processes pertaining to human physiology is then discussed under two broad categories of bio-mass and bio-heat transport. The bio-mass transport section discusses LDL transport in arteries, drug delivery, drug eluting stents, functions of organs modelled as porous medium, porous medium modelling of microbial transport. Under the bio-heat transport section, porous medium approach based bio-heat equations are described accompanied by a literature review. A final subsection discusses non-Fourier type bio-heat conduction phenomena. Requirement of analysis and computational efforts in the future using the generalized porous medium momentum equation and the local thermal non-equilibrium based two energy equations are highlighted.

*Department of
Mechanical Engineering,
Indian Institute of
Technology Madras,
Chennai 60036, India
arunn@iitm.ac.in*

1. Introduction

Bio means Life. Bioengineering, “an essential underpinning field for the 21st century”, according to the US-NSF and NIH, applies engineering principles and laws of physics, chemistry and mathematics in a general sense, to the understanding and modelling of living systems. Biotechnology identifies methods, processes and techniques resulting from bioengineering. Examples of bioengineering driven technology range from micro-scale applications such as genetic engineering to macro-scale designs such as artificial lungs and tissues.

Biothermology or Bioheat transfer and bio-mass transfer can be seen as a subdivision of

bioengineering. The three-fold objectives of heat transfer, viz. insulation, enhancement and control of temperature, when applied in the context of biological systems, offer insights into many biological processes. Examples of bioheat transfer processes specific to humans include:¹

1. Thermoregulation; metabolic heat generation, evaporation, convection and radiation to achieve steady state;
2. Effect of increased Metabolic Heat Generation; temperature rise during exercise
3. Bioheat transfer in muscles and tissues accompanied with effects due to blood flow (perfusion)

Keywords: Bio-fluid dynamics, Bio-heat transfer, porous medium, arterial flow, drug delivery, drug eluting stents, tissue modelling, tissue ablation, thermotherapy, laser surgery.

4. Burning; skin burning as transient heat transfer process
5. Fever and Hypothermia
6. Thermal Comfort; Convection, conduction heat transfer through clothing, optimum temperature, humidity, energy transfer in artificial fittings like contact lens

Similarly, mass transfer studies, within the purview of biology, helps in understanding several bio-mass transfer processes that can be identified within the human body:

1. Blood as oxygen carrier; equilibrium of oxygen in blood with inhaled air
2. Metabolism; diffusive oxygen transfer in a tissue
3. Membranes as barriers to bulk flow; diffusive and ionic flows through membrane channels; porous medium models of capillaries and tissues
4. Liquid Diffusion in tissues; drug delivery to local regions inside body; diffusion of gastric juice in the stomach

Computer modeling and simulation is critical in the field of bioengineering where experimental verification is inherently complex owing to lack of easy accessibility of functional biological organs, their complex geometries and in general, the prevailing safety regulations. Computational bio-fluid flow and bio-heat transfer studies have become an important tool for investigation of complex biophysical phenomena difficult or impossible for experimental observations. Advances in simulation and modeling aids, hardware and software improvements and interdisciplinary knowledge have made it feasible to apply the computational paradigm to biological systems. Bioengineering computational models are typically either bionic (designing bioengineering systems) or mechanobiological (understanding basic processes). As a thermal engineer would expect, modeling of biofluid dynamics forms an inherent part of the subsequent bioheat transfer, when convection or conjugate heat transfer are to be investigated.

The porous medium modelling approach, now an established methodology in other engineering disciplines, has made forays into biomechanical modelling over the past two decades. Many biological systems involving multi constituents can readily be approached as porous media for simplified analysis. An obvious example of mass transport in biological systems that can be modelled as porous medium is the diffusion of

nutrients and other macromolecules (drugs etc.) across and within biological tissues. An earlier review by Khaled and Vafai² describes studies carried out prior to 2002 on porous medium models used in specific biological and biomedical applications such as tissue generation in scaffolds, transport in brain tissues, MRI applications, liquid chromatography, transport of macromolecules in aortic media, blood flow through muscles, and interstitial fluid flow in axi-symmetric soft connective tissue. Porous medium models are applicable to mass diffusion across tissues because tissues are classic three-dimensional porous media composed of dispersed cells and fibres separated by connective voids, through which interstitial fluids circulate. In fact, the porous medium theory is applicable at various scales in biological systems—organ, tissue, macro, micro, nano, and cells can all be represented as porous media.²⁻⁴

Before elaborating on available literature on the modeling of biological systems as porous media, for self-consistent reading and completeness, we shall recount briefly the basics of porous medium modelling along with the rudimentary conservation equations involved.

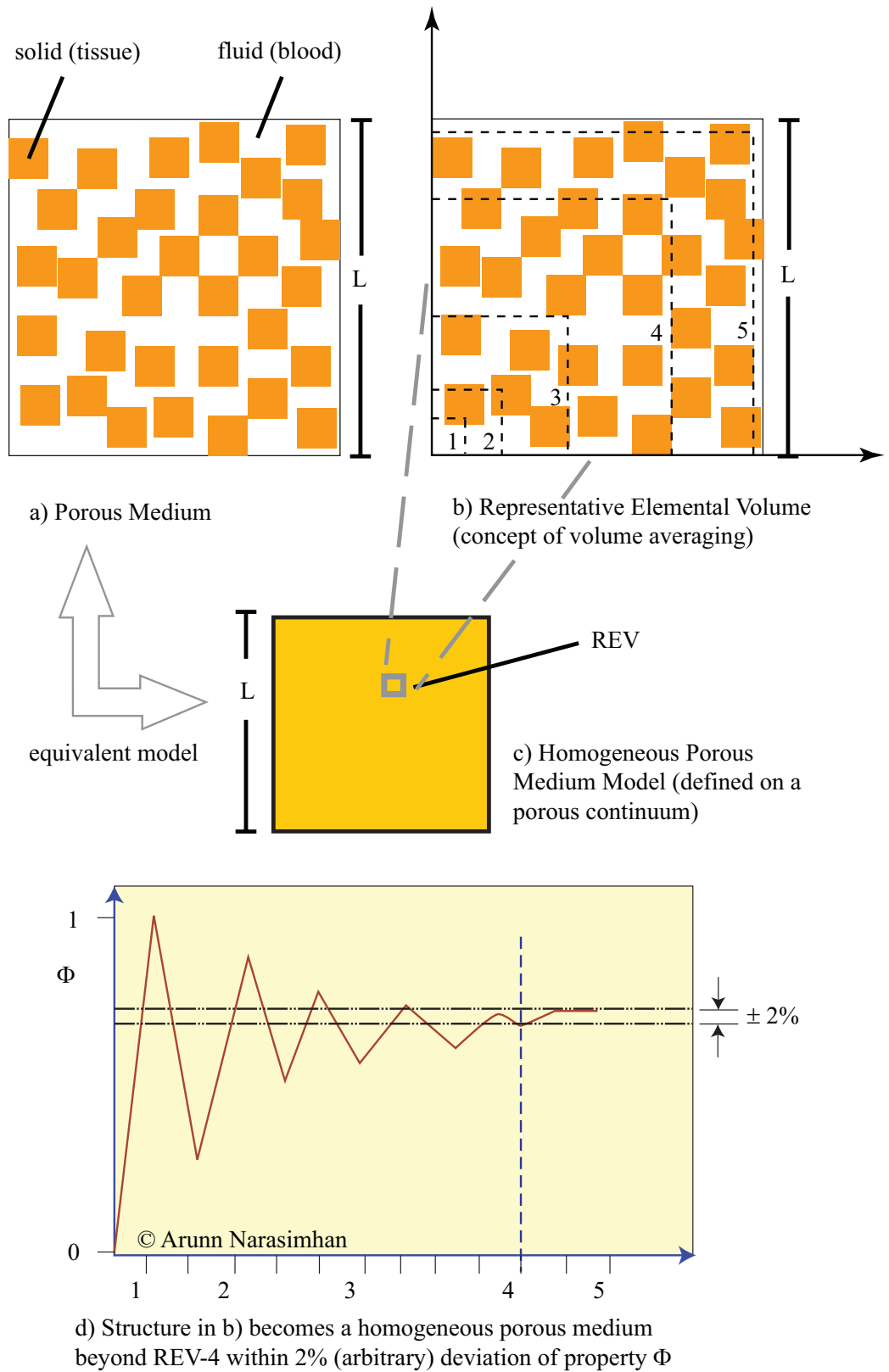
2. Porous Medium Concepts

A definition for porous medium, suited for analysing transport phenomena, is a region in space comprising of at least two homogeneous material constituents, presenting identifiable interfaces between them in a resolution level, with at least one of the constituent remaining fixed or slightly deformable. It is usually characterized by a volumetric porosity (ϕ) and permeability (K, m^2).

Central to analysing heat and fluid transport through porous media is the idea of volume averaging that renders the porous region into an equivalent homogeneous space suitable for continuum analysis. Analogous to the continuum concept defined for single constituents, a homogeneous porous medium is defined over a porous continuum. Every point in the porous continuum represents, not the individual solid or fluid constituents, but the combined porous medium. Such a porous continuum point represents a finite volume of the porous medium called the Representative Elemental Volume (REV). This procedure is explained in the schematic of the figure.

In this context, microscopic scale refers to the micro level of the individual solid or fluid constituent of the porous medium (within the individual constituents in Fig. 1a), while macroscopic scale refer to the coarser combined region of solid and fluid of the porous medium

Figure 1: Porous Medium: a) definition b) volume averaging and REV c) homogeneous porous medium model d) determination of homogeneity for property Φ of porous medium.



at the representative elemental volume level (Fig. 1c). The global scale refer to the larger length scales of the finite volume of the porous medium (L), where experimental measurements result in the determination of porous medium properties like permeability and form coefficient. A biological region formed by tissue irrigated by blood flow is a porous medium at the global scale and the representative elemental construct containing finite small blood and tissue volume is the macroscopic scale, while the region within this REV can be at the microscopic scale.

The picture of the porous medium in the figure, viewed from afar, would blur the interfaces between the metal matrix and the voids, resulting in a continuous indistinguishable haze. Such a coarser visual resolution (or equivalently, the sample size) is essential for treating a region suitable for volume averaged porous medium analysis. Alternately, such a homogeneous porous medium approach provides useful results when the representative pore size of the porous medium is much smaller (usually three orders) than the largest length scale of the domain of interest. Sweating from skin, for instance, can be investigated using a porous medium modelling approach, when the individual sweat pores are sufficiently small and many in a much larger human skin surface.

2.1. Flow Through Porous Medium

The filter-like picture shown in Fig. 2 represents the filtration experiments carried out by Henry Philibert Gaspard Darcy in Dijon, France in the middle of the 19th century, when he was working there as the “Dean of the School of Bridges and Roadways” and was involved in planning the fountains of the city of Dijon. While working on filtering hospital waste water, Darcy described his empirical studies [ref] on steady-state filtration in detail. He demonstrated with his experimental results that the watervolume passing through a sand layer is proportional to the pressure-drop across the length of the layer, leading to the equation.

$$\alpha = U / (\Delta P / L) \quad (1)$$

where α is the hydraulic conductivity of the porous medium, U is the channel cross-section averaged fluid speed, also known as the seepage speed, and ΔP is the hydrostatic pressure difference (i.e., inlet minus outlet) across the porous medium layer of length L .

Darcy’s equation, as proposed, is an algebraic equation involving cross-section average quantities. That is, it is not the differential

momentum conservation equation but a solution to one with prescribed boundary conditions. Darcy Law involves global quantities, which can be measured—as Darcy did—in an experiment. The α in the original Darcy law later was distilled by researchers as a ratio of the fluid dynamic viscosity and a specific permeability, a property of the porous medium through which the flow happens. This would make Eq. (1) read in today’s context as

$$\frac{\Delta P}{L} = \frac{\mu}{K} U \quad (2)$$

The important contribution of Darcy’s 1856 paper is perhaps the recognition of permeability, K, m^2 , as a porous medium property, in its primitive form. It took a few twists and turns and adhoc extensions to evolve a differential momentum equation for which the above Darcy law is a solution. The relevant history is summarized in the schematic of Fig. 2. Figure 2 essentially traces only the concepts originated through experiments, in other words, the modelling of flow through porous media done at the global scale. Further historic details are available in the excellent review by Lage.⁵

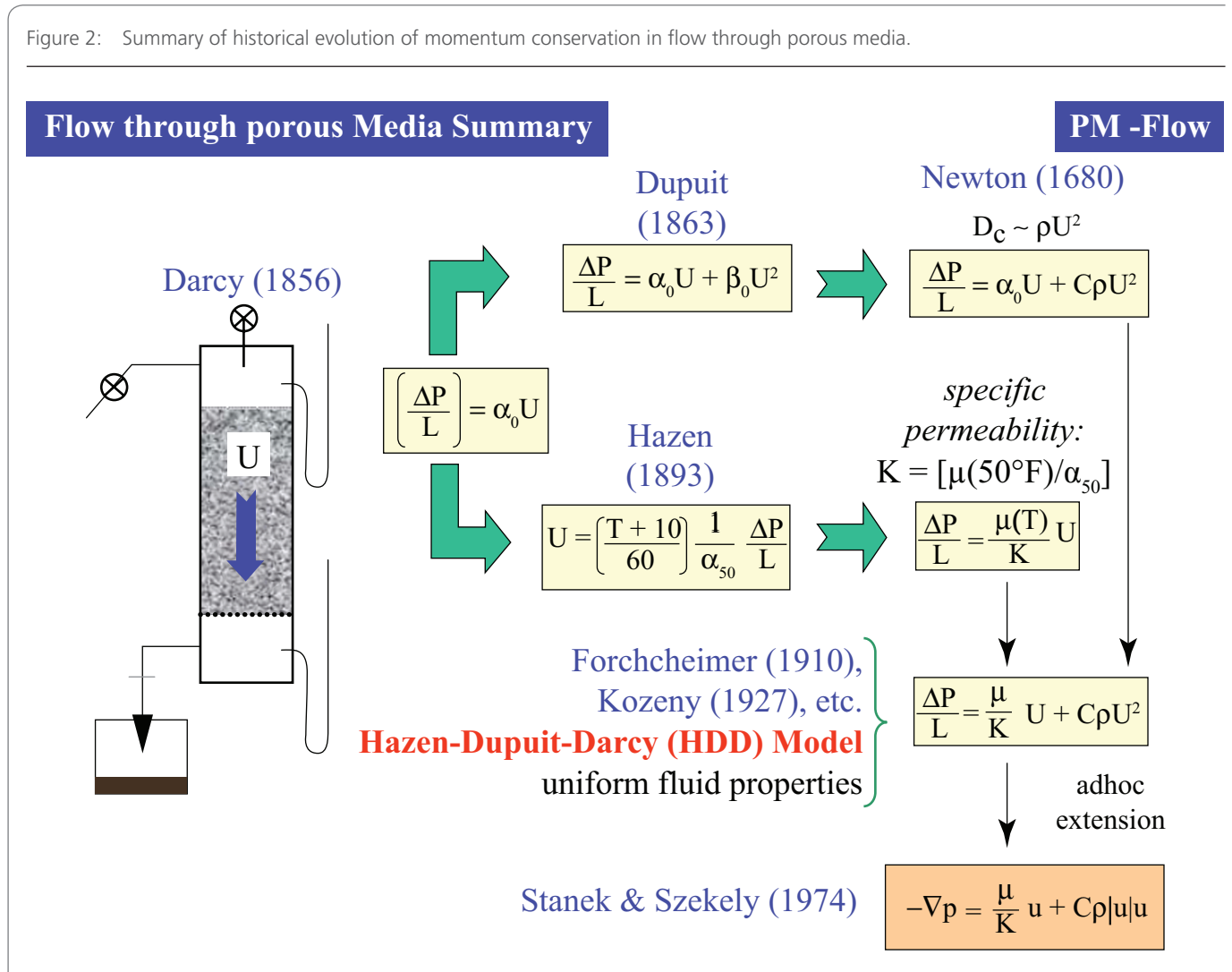
A step towards the generalization of Darcy’s equation valid at a global scale for the porous medium, is the ad-hoc extension of the global Hazen-Dupuit-Darcy model into the differential form

$$-\nabla p = \frac{\mu}{K} \bar{u} + \rho C |\bar{u}| u \quad (3)$$

where \bar{u} is the Darcy velocity, also known as the local (macroscopic, or representative elementary volume) seepage fluid velocity. It is related to the intrinsic pore average velocity as $\bar{u} = \phi u_p$, where $u_p = \int u(x, y) dA$, the integral taken over the local pore cross section in an REV of a porous medium. The ∇p in Eq. (3) is the local (macroscopic) pressure gradient, related to the pore cross-section averaged static pressure by $p = \phi p_p$. The two terms in the RHS of Eq. (3) represent the lumped viscous and lumped form effects (forces) within the macroscopic permeable medium and are usually designated as viscous drag and form drag respectively, as they impede the flow.

Ideally, if one were to perform a volume integration of the differential momentum equation, Eq. 3, (also shown in the bottom orange box in Fig. 2), it should lead to a result similar to that of the, experimentally verifiable, global momentum conservation equation just above it (yellow box) in Fig. 2. The schematic in Fig. 2 doesn’t provide a complete picture of the modelling challenges

Figure 2: Summary of historical evolution of momentum conservation in flow through porous media.



involved in the differential scale or the macroscopic or pore level modelling of the porous medium. Also, the schematic captures only the evolution of the global momentum conservation statement for a particular restricted class of porous media partly due to the nature of the earlier experiments done (in the 19th and early 20th centuries) to understand the flow through porous media, which involved mostly low permeable media ($K < 10^{-7} m^2$) like sand filters.

A more general representation of the macroscopic momentum model, Eq. (3), which includes other force terms is given below.

$$\rho_f \left[\frac{1}{\phi} \frac{\partial u}{\partial t} + \frac{1}{\phi} u \cdot \frac{1}{\phi} \nabla u \right] = -\nabla P + \mu_{eff} \nabla^2 u - \frac{\mu}{K} u - \rho C |u|u \quad (4)$$

The ϕ in the above equation represents the volumetric porosity of the porous medium

(total pore volume divided by the total volume of the porous medium); P , Pa and u , ms^{-1} are the cross section averaged static pressure and velocity (vector) at the REV level. The μ , Nsm^{-2} and ρ , kgm^{-3} are the dynamic viscosity and density of the fluid that flow through the porous medium while K , m^2 and C , m^{-1} are the hydraulic properties permeability and form coefficient of the porous medium. The form coefficient is further related to the permeability as $C = c/\sqrt{K}$, where c is a dimensionless constant that could vary depending on the porous medium.

Equation (4) has six physical properties of which ρ and μ can be obtained as measurements using their separate constitutive relations. Porosity ϕ can be determined independently. The other porous medium hydraulic properties permeability K , form coefficient C and effective viscosity μ_{eff} depend on the geometry of the permeable medium. Unique constitutive relations doesn't exist for their determination and

hydraulic experimental data needs to be matched with solutions to the above momentum equation, Eq. (4), for individual porous medium. The difficulty of this procedure only gets amplified for bio-materials, requiring internal access to organs with complex geometries desired to be modelled as porous media.

Equation (4), identified on occasion as the generalized Navier-Stokes equation, is recognized as the most general momentum conservation statement for porous medium flows. It is valid on a porous continuum, a continuous space whose differential 'point' is in principle equivalent to the REV of the actual porous medium being modelled (see Fig. 2). The first additional force term $\mu_{eff} \nabla^2 u$ arises due to the Brinkman effect, the fluid-fluid viscous shear ever present in a viscous flow and which is a distinct force from that of the internal fluid-solid viscous drag present in the porous medium flows (identified as Darcy or viscous drag). Accordingly, $\mu_{eff} Nsm^{-2}$ is identified as the effective viscosity, a quantity believed to be a function of the geometry of the porous medium at the REV level and hence, is often related to the volumetric porosity as $\mu_{eff} = \phi^{-1} \mu$. The other included force, the second term on the LHS, is due to the convective inertia. A comparative summary of the nature of the force balances in the momentum conservation of various flows within and without porous media is given in the schematic of Fig. 3.

The Brinkman effect manifest dominantly only for coarser porous media with volumetric porosity $\phi > 0.6$.⁶ Such porous medium modeling has been used to understand biological processes like pathological blood flow when accumulations of fatty plaques of cholesterol and artery-clogging blood clots increase in the lumen (the cavity or channel within a tube) of the coronary artery.² The convective inertia for porous medium flows is usually negligible when compared to the other dominant drags present due to the porous solid matrix. This observation holds also for several of the biological processes that could be modelled as porous medium flows.

2.2. Energy Balance in Porous Medium with LTE Assumed

In Fig. 4, a sample parallel plate bounded porous medium convection region is modelled as a homogeneous one dimensional heat and flow configuration. The Darcy law in its global and differential form (text inside the green box in Fig. 4) is taken to govern the momentum conservation in this particular case. The surface porosity is invariant in the x direction and hence equal to the volumetric porosity ϕ .

Since atleast one solid and one fluid phase is involved in constructing a porous medium, the energy balance requires the conservation of energy transfer that could prevail in and between these two phases. Hence, in principle, two energy equations, one each for each of the material constituent, needs to be solved with a proper interfacial energy flux closure. Nevertheless, the energy balance is the first law of thermodynamics, applied on an open system where mass and energy are allowed to 'cross' the boundaries that separate the system from its surroundings.

The two energy equations can be written as
Solid side

$$(1 - \phi)(\rho c)_s \frac{\partial T_s}{\partial t} = (1 - \phi) \nabla \cdot (k_s \nabla T) + (1 - \phi) q''' \quad (5)$$

Fluid Side

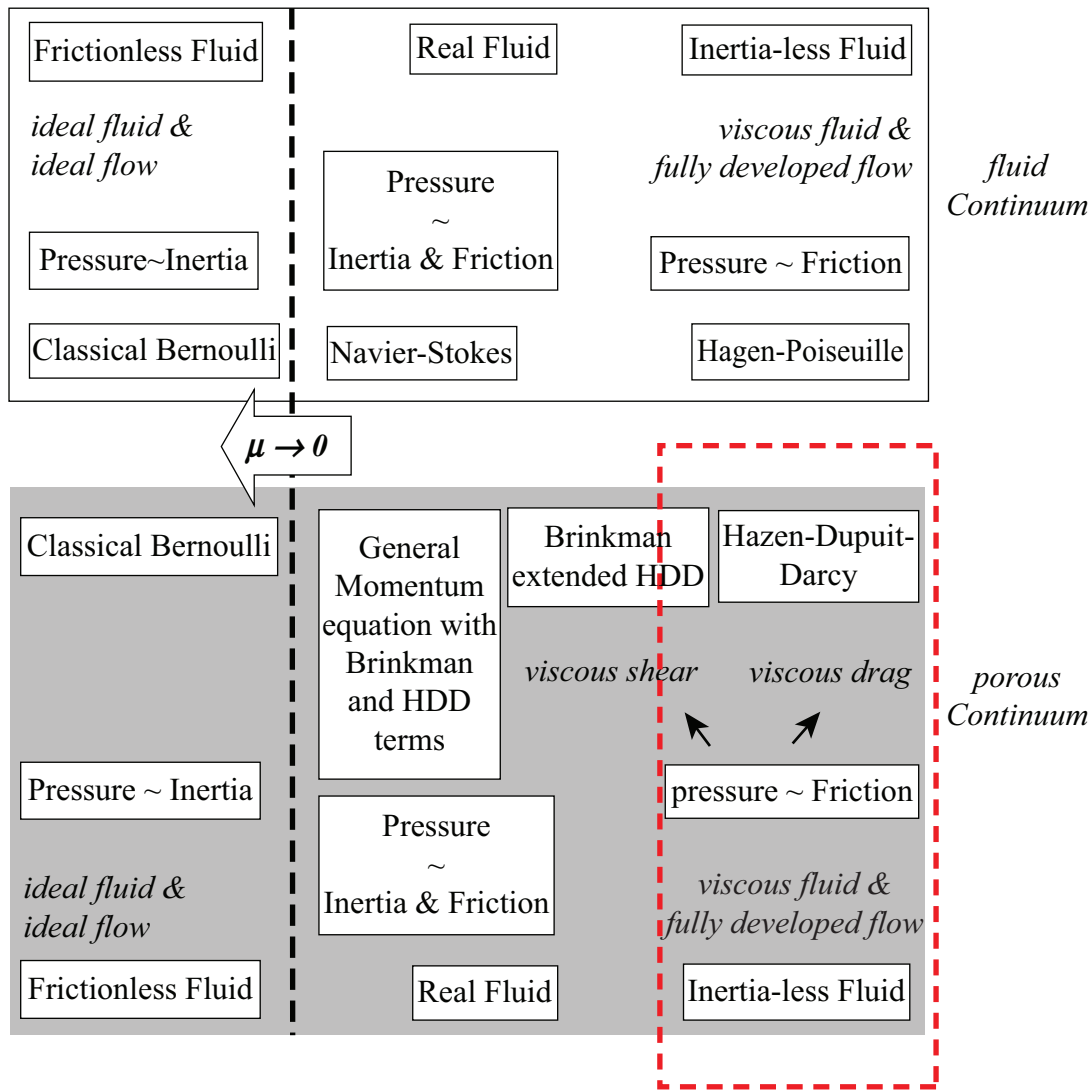
$$\begin{aligned} \phi(\rho c_p)_f \frac{\partial T_f}{\partial t} + (\rho c_p)_f \vec{v} \cdot \nabla T_f \\ = \phi \nabla \cdot (k_f \nabla T_f) + \frac{\mu}{K} v^2 \end{aligned} \quad (6)$$

Observe that the fluid side by the volumetric porosity ϕ while the solid side is 'weighted' by $(1 - \phi)$ and the velocity in the fluid side is cross section averaged, i.e. $v = \phi v_p$, as discussed beside the momentum equation. The volumetric internal heat generation is present only in the solid side (the last term in Eq. (5)) and the viscous dissipation term is present only in the fluid side (the last term in Eq. (6)). Also, the viscous dissipation is modelled as the power required for the fluid to "extrude" itself over the porous solid structure. This is equivalent to the pressure drop in the Darcy form of the momentum conservation times the seepage speed Eq. (1), resulting in an expression of the form given as the last term in Eq. (6).

If one were to solve these equations separately, an interfacial closure term involving a local convection heat transfer coefficient is required (absent in Eqs. (5) & (6)) that account for the local heat transfer between the solid and the fluid flow. Omission of this term in above two equations is possible with the assumption that the temperature of the solid and the fluid inside a REV is identical. In other words, local thermal equilibrium between the solid and the fluid is assumed at the REV level while writing Eqs. (5) and (6).

From Fig. 4 it is obvious that the one-dimensional porous medium convection configuration is a parallel arrangement at the REV level. Invoking the volume averaging concept and combining the above two equations to obtain a single energy

Figure 3: Schematic of delineation of flows using force balance without and within porous media.



equation and generalizing for three-dimensions using vector notations would result in:

$$(\rho c_p)_f \left(\sigma \frac{\partial T}{\partial t} + v \cdot \nabla T \right) = k_e \nabla^2 T + q''' + \frac{\mu}{K} V^2 \quad (7)$$

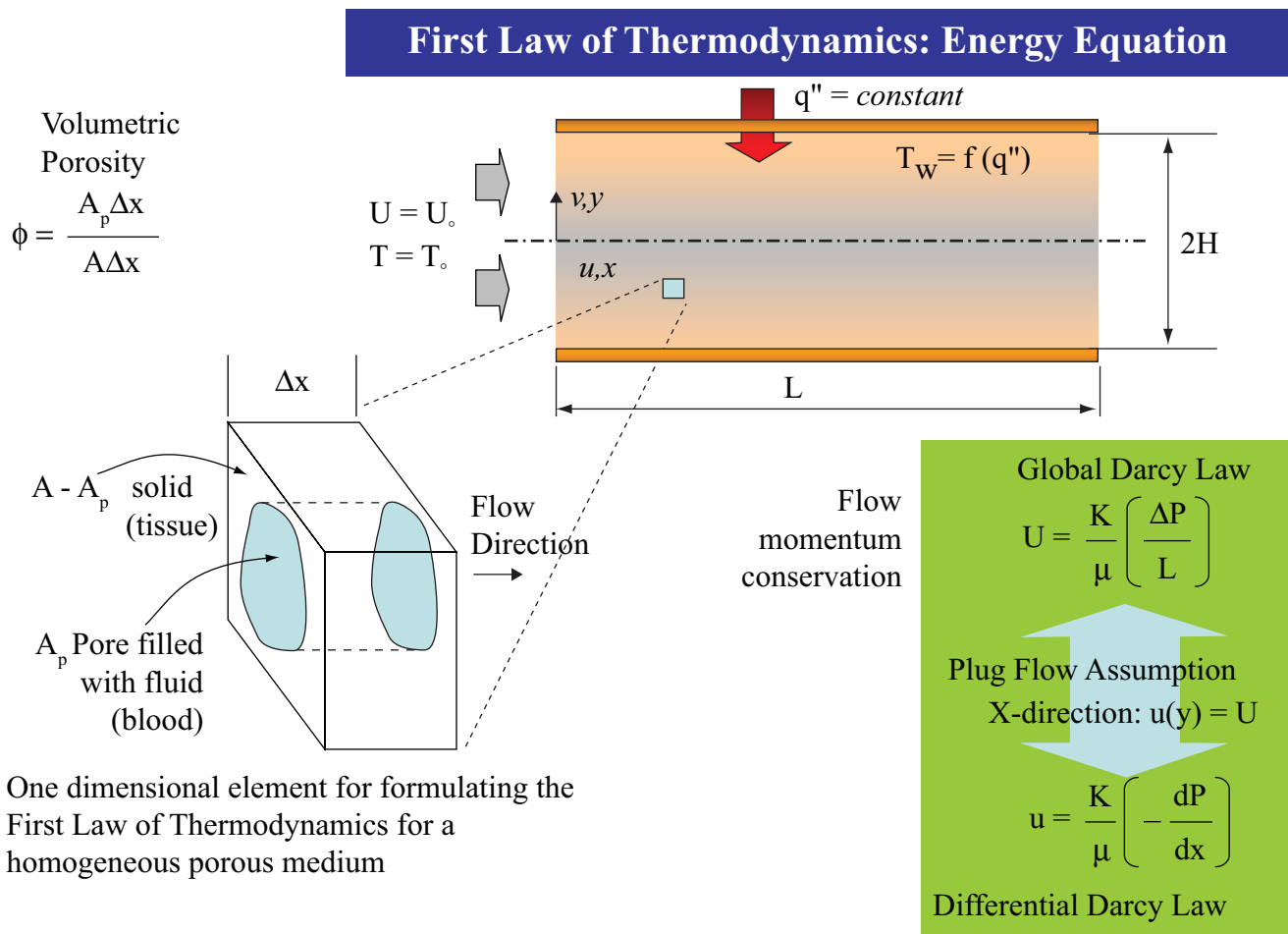
The temperature T present in Eq. (7) is neither the temperature of the solid nor that of the fluid but is that of the porous medium. The effective thermal conductivity k_e and effective thermal capacitance σ owing to the parallel arrangement of the solid and the fluid flow in the REV level, can be defined as $k_e = \phi k_f + (1 - \phi) k_s$ and $\sigma = (\phi(\rho c_p)_f + (1 - \phi)(\rho c_p)_s) / (\rho c_p)_f$ respectively. Other functional relationships are possible depending on the nature

of the geometry of the investigated porous medium (readers may consult Chapter 3 in).⁶

Some of the major assumptions in writing the volume averaged energy conservation statement in Eq. (7) are as follows: 1) homogeneous porous medium 2) local thermal equilibrium between the solid and the fluid of the porous medium exists in the REV level itself. 3) effective properties used in the volume averaged energy equation are accurate in predicting the effects in the REV level. 4) the rest of the primitive variables, u , P and T are volume averaged quantities defined on a porous continuum.

In the next sections we shall review literature pertaining to bio fluid and heat transport processes modelled primarily using the porous medium

Figure 4: Volume averaged energy balance statement for porous media when local thermal equilibrium prevails between solid and fluid phase.



concepts discussed in this section. Literature published after 2003 only is discussed with some detail as other excellent reviews of related topics cover much of the related published literature before 2003. The reader is directed to² and⁴ and also to¹ for bio heat transfer models.

3. Porous Medium Modelling in Bio-mass Transport

We shall now discuss some specific examples of the use of porous medium modelling in understanding mass flow in biological systems.

3.1. LDL Transport Across Arterial Tissues

Plaque, the build up of fatty substances, cholesterol, cellular waste products, calcium and other substances on arterial walls, resulting in Atherosclerosis, is a direct result of transport of the low-density lipoprotein (LDL) among other macromolecules, from the blood through the

arterial wall. Given the seriousness of the disease, there has been considerable interest in recent years on modeling the transport of macromolecules such as LDL across arterial walls.⁷ Comprised of four layers—endothelium, intima, media and adventitia—the arterial wall is a typical porous medium and relevant parameters such as permeability and porosity of wall, velocity of blood, arterial pressure, pulsatile behavior of flow are available in literature to enable modeling of the LDL transport across the wall as a flow across porous medium problem.

Studies on macromolecular transport across arterial walls has been classified by Prosi and coworkers⁹ into three categories—wall-free models, fluid wall (or homogenous wall) models and multilayer models developed by Karner.¹⁰ While the first two are simplistic models that use minimal parameters, they are far removed from realistic situations. The multilayer models

represent transport across many distinct layers of the wall at the microscopic or macroscopic levels.

Sun and coworkers¹¹ used the homogeneous-wall model to understand the effects of wall shear stress on the mass transport from blood to and within the wall of a stenosed artery under steady conditions. They used the Navier Stokes and advection diffusion equations to model flow and species transport in the lumen and Darcys law to solve the transmural flow in the arterial wall. They coupled the mass transport within the artery with the transmural flow to obtain the species distribution across the arterial wall. A homogenized model was also used by Olgac and coworkers¹² in a patient-specific three-dimensional simulation of LDL accumulation in a human left coronary artery in its healthy and atherosclerotic states. They showed that in the diseased state, the site with high-LDL concentration shifted distal to the plaque, which is in agreement with the clinical observation that plaques generally grow in the downstream direction.

The multilayer model has been most frequently used in recent years as it provides a more realistic picture of the arterial structure. This model shows that the occurrence of smooth muscle cells in intima and the metabolic processes in media create a concentration gradient across the layers and hence govern the macromolecular concentration. Tada and Tarbell¹³ used a layered arterial wall model, consisting of internal elastic lamina and medial layers alone, to analyse the effect of the internal elastic lamina (IEL) on macromolecular transport of LDL and adenosine triphosphate (ATP) molecules in the arterial wall. The concentration gradient was produced by uptake of macromolecules by smooth muscle cells. These studies showed that the IEL pore structure

greatly affected the ATP and LDL concentration in media. ATP transport was governed by diffusion whereas, LDL transport governed by convection. It was concluded that the diffusion driven transport of molecules, responsible for intimal hyperplasia, depends on IEL pore structure.

Sun et al. have also studied the influence of wall shear stress and transmural pressure on LDL accumulation in arterial wall using the multilayer model.¹⁴ Low wall shear stress and high transmural pressure lead to increased accumulation of LDL in the arterial wall. They also studied the influence of pulsatile flow on LDL transport and showed that a steady flow assumption was inadequate to simulate transport of LDL in arteries that see complex flows, especially those near bifurcations.

Olgac and coworkers also studied the effect of wall shear stress on LDL accumulation using a three-pore model and obtained results similar to Sun's [?]. Olgac suggested that transport of macromolecules takes place through three types of pathways viz. sites of dying cells, normal porous region and transcytosis (selective transport of macromolecules from one side of cell to the other). The three-pore model represented the dependence of blood plasma and LDL transport through the endothelium on the local blood flow characteristics better than the single pathway approaches of Sun et al.¹⁵

Prosi et al. also used a multi-layer model composed of endothelium, intima, IEL, and media to solve the Navier Stokes equation and the advection diffusion equation to obtain the flow and concentration fields within the lumen.⁹ Darcys law was coupled with a species equation for the transport process. It was shown that the wall thickness and curvature influence the concentration profiles of LDL. The results of multilayer model were consistent with fluid-wall models for same set of input data.

Ai and Vafai studied the effects of hypertension and geometrical variation on the LDL accumulation within the wall using advection diffusion equations in porous media in the multilayer model.¹⁶ In another study, Yang and Vafai used a finite element scheme based on the Galerkin method of weighted residuals in the four-layer model to describe the LDL transport in the arterial wall coupled with the transport in the lumen.⁷ They also studied the effects of pulsatile flows on LDL transport in the arterial wall. In all these studies, blood was considered to be a Newtonian fluid and the artery was assumed to have rigid boundaries. Their studies described the concentration profiles of LDL in the arterial wall.

Khakpour and Vafai¹⁷ analysed and reviewed papers on arterial transport porous medium models

Figure 5: Plaque in human artery.⁸



used to study fluid flow and mass transfer within the arteries. They have also performed numerical simulations of the macromolecule transport at the aortailiac bifurcation using a four-layer porous wall model.¹⁸ The layers are treated as macroscopically homogeneous porous media with uniform morphological properties. High concentration of LDL at the lumen endothelium interface has been shown to play a key role in the development of atherosclerosis. This study also reported the effects of gender and geometrical characteristics (e.g. asymmetry) on the LDL transport phenomena at the aortailiac bifurcation—both wall shear stress and wall macromolecule concentration profiles were found to be more uniform in an average male geometry than at the female iliac bifurcation.

Koshiha et al.¹⁹ modelled a deformable arterial wall using a porohyperelastic model (PHEM) to express both the filtration flow and the viscoelastic behavior of the living tissue, and simulated a blood flow field in the arterial lumen, a filtration flow field and a displacement field in the arterial wall using a fluid-structure interaction (FSI) program code by the finite element method. They further simulated LDL transport using a mass transfer analysis code by FEM and compared the porohyperelastic model to a rigid model. In the porohyperelastic model, the maximum LDL concentration in the wall in the radial direction was observed at a position of 3 percent wall thickness from the lumen/wall interface, while for the rigid model, the LDL concentration peaked at the lumen/wall interface. In addition, the peak LDL accumulation area of the PHEM moved according to the pulsatile flow. Their results demonstrated that that the blood flow, arterial wall deformation, and filtration flow affect the LDL accumulation. Badia and coworkers have coupled the Biot and Navier Stokes equations to model fluid poroelastic media interaction during mass transport from the arterial lumen to the arterial walls and inside the walls.²⁰

3.2. Mass Transport in Tissue Regeneration

Tissue engineering is an emerging technology for treatment of a variety of orthopedic and muscular maladies. It involves the application of biological, chemical, and engineering principles toward the repair, restoration, or regeneration of living tissues using biomaterials, biomimetic materials and cells.²¹ Three dimensional porous scaffolds are being increasingly used as the substrate for cell culture and attachment and tissue organization in bone regeneration—an *in vivo* “bioreactor”. Such scaffolds are characterised by good porosity for nutrient transport, biocompatibility and good mechanical strength. Scaffolds are typically

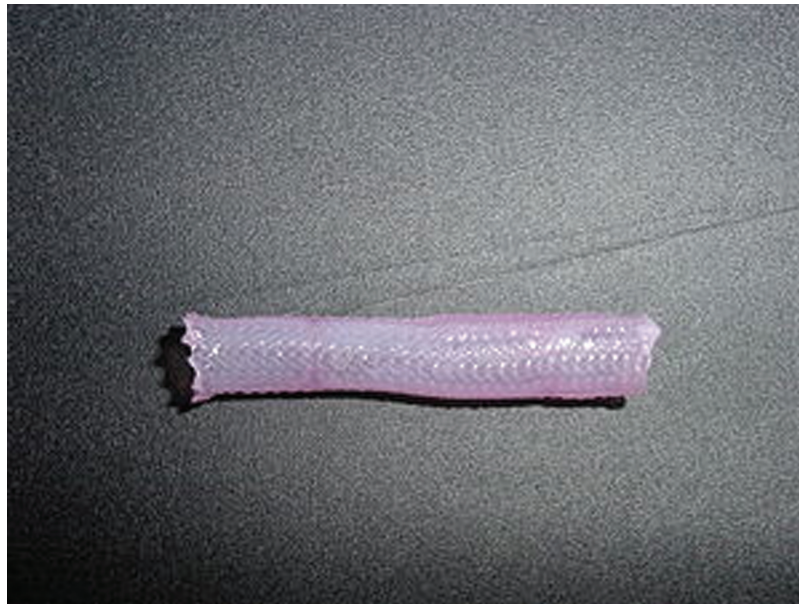
made of natural materials such as collagen, glycosaminoglycan and chitosan or synthetic polymers like polyglycolic acid (PGA), polylactic acid (PLA), and polycaprolactone (PCL).

The properties of tissue engineered scaffold matrices are critical for safety and long-term clinical success of the scaffold. An ideal scaffold should provide a suitable environment for nutrient delivery, waste removal, and mechanical stimulation, thus necessitating high porosity and permeability. It is therefore important to understand their mass transport properties. The scaffolds may be considered porous media though which there is a flow (“perfusion”) of homogeneous fluid and may be related to flows with simple geometries, such as flow over a porous layer or flow through a porous plug.

Lasseux and coworkers derived a macroscopic model to describe reaction and transport by diffusion and convection of two species within a porous medium, a situation seen during *in vitro* tissue growth.²³ The tissue at the microscopic scale was treated as a three phase structure in which solid polymer fibres were explicitly taken into account as a separate phase in addition to the cell phase and fluid phase. Convective transport was considered in the fluid phase in addition to the classical diffusive transport and the volume averaging method was used to develop a macroscopic one equation model.

Porter et al. applied the Lattice Boltzmann method to simulate the culture media flowing through scaffolds in a bio-reactor.²⁴ This modeling compared results for different perfusion bioreactor systems or different scaffold microarchitectures and could allow specific shear stresses to be determined for optimization of the amount, type, or distribution of *in vitro* tissue growth. Costa et al. proposed a control-volume finite element method to simulate the problems of coupled viscous and porous flows, assuming continuity of both velocity and stress at the porous fluid interface.²⁵ Betchen et al. introduced pressure velocity coupling to develop a similar finite volume model.²⁶

Boschetti and coworkers characterized through CFD studies, the hydrodynamic field imposed to cells in a micro-porous scaffold.²⁷ The variation of the local shear stress distribution was evaluated as a function of parameters that can be controlled during the scaffold fabrication process, such as the scaffold porosity and the pore size, and during the cell culture, such as the medium flow rate and the diameter of the perfused scaffold section. For a given pore geometry, the pore size was found to strongly influence the predicted shear stress level, whereas the porosity strongly affected the

Figure 6: Engineered Vascular Tissue.²²

statistical distribution of the shear stresses but not their mode value. The results of the simulations indicated that low porosities allow a better control of the shear stress level imposed to the cells.

Adachi and co-workers proposed a framework for the optimal design of the porous scaffold microstructure by three-dimensional computational simulation of bone tissue regeneration involving scaffold degradation and new bone formation.²⁸ The voxel finite element method was applied to simulate the bone regeneration process in a bone scaffold system. The regeneration process was quantitatively evaluated by measuring the change in the strain energy of the bone scaffold system. Case studies for scaffolds with lattice-like and spherical pore structures were carried out, and demonstrated the applicability of the design of the porous scaffold microstructure.

Coletti et al. developed a mathematical model of convection and diffusion in a perfusion bioreactor, combined with cell growth kinetics.²⁹ The model described the spatio-temporal evolution of oxygen concentration and cell density within a 3D polymeric scaffold. The fluid dynamics of the medium flow inside the bioreactor was described using the Navier-Stokes equations for incompressible fluids. The convection through the scaffold was modelled using the Brinkman porous medium model, i.e. steady state version of Eq. (4) without the convective inertia and the form drag terms. The study showed that convection, diffusion,

and cell growth depend strongly on the properties of the scaffold, such as porosity and permeability, which change in time and space.

Chung and co-workers developed a mathematical model to simulate nutrient flow through cellular constructs by treating them as a biphasic porous medium consisting of the void fluid phase (culture medium) and the full cell phases.³⁰ The cells and extracellular matrix were treated as a single unit. The model incorporated modified Contois cell-growth kinetics that contains nutrient saturation and limited cell growth rates. Numerical simulations showed that cells penetrated to a greater extent into the scaffold and resulted in a more uniform spatial distribution when cells were cultured under direct perfusion. It was shown that perfusion also imposed flow mediated shear stress to the engineered cells.

Sans Herrera et al. proposed a coupled micro macro numerical approach where the effective scaffold properties required at the macroscopic scale are derived from the asymptotic homogenization theory and the microscopic variables are obtained by solving the associated localization problem.³¹ They derived the macroscopic Darcy's law for an incompressible viscous fluid flowing in a porous medium. A model for bone in growth at the microscopic scaffold surface was proposed considering the strain energy as mechanical stimulus. The model provided information on bone formation distribution at scaffold evolution

of the macroscopic diffusion coefficient and mechanical properties considering anisotropy due to the effect of bone regeneration and the evolution of the scaffold microstructure at each point of the scaffold domain.

Yu and coworkers applied numerical simulations to predict the fluid dynamics and oxygen transport inside a micro-bioreactor for animal cell culture.³² The scaffold structure and cells attached on the scaffold were considered the porous medium. The velocity around the top surface of the scaffold was higher at a higher Reynolds number and the flow approached the scaffold more perpendicularly. High porous flow was also observed within the scaffold with an increase in Reynolds number.

Whittaker et al. developed a simple mathematical model based on Darcy's law for forced flow of fluid (culture medium) through a porous scaffold.³³ In this model, porous-walled hollow fibres penetrate the scaffold and act as additional sources of culture medium. The model helps design effective experiments by estimating the range of flow rates required to achieve a desired shear stress distribution and ensure sufficient nutrient and waste transport. The model can also predict how often the culture medium needs to be replenished during the culturing.

3.3. Drug Delivery

The clinical relevance and importance of drug administration cannot be understated. The effective release of active pharmaceutical ingredients from delivery vehicles (pills, injections, transdermal patches etc.) to the target tissues decides the efficacy of the pharmacological treatment. Mathematic modelling has enabled drug delivery/administration to evolve from the passively pre-programmed activity of the past to a dynamic self-programmed activity. Drug delivery is controlled by the rate-controlling release mechanism such as diffusion, erosion/chemical reactions, swelling and osmosis. The drug is often distributed in a matrix that can either be nonporous/homogeneous or porous/granular. When the matrix is porous, diffusion of the drug is restricted to pores in an otherwise impermeable material. Diffusion is usually the rate determining step in such systems, but drug release can also occur through processes such as matrix swelling and erosion. In transdermal patches, convection is the leading drug transport mechanism.

Computational fluid dynamics simulation can predict the spatial and temporal variation of drug transport in the living tissues. Macroscopically, the tissue can be assumed as an isotropic porous medium. The drug transport in the tissue can be

assumed to be a combination of convection and diffusion in the porous medium. Thus the concept of percolation theory for the solute transport in the porous medium can be applied with additional feature of solute elimination kinetics.³⁴

Transcleral drug delivery is used to treat a variety of eye diseases such as age related macular degeneration, and involves placing the drug at the posterior section of the eye. Several recent studies of transscleral drug delivery have attempted to derive pharmacokinetic models to explain the transfer rates of the drug through the posterior eye tissues.³⁵⁻³⁷ Ranta et al.³⁸ reported a pharmacokinetic simulation model based on the scleral permeability coefficient P_s , which accounts for circulation loss and predicts the overall permeation flux through the sclera. Ram and coworkers recently reported a 3D porous medium approach using finite element method for studying transscleral drug delivery,³⁹ which accounted for the diffusion and convection losses, assuming linear effect of choroidal blood flow on the drug delivery.

Narasimhan and Ramanathan have recently developed a porous medium model of sclera and choroid to study the effect of choroidal blood flow on transscleral delivery of the drug anecortave desacetate, to the retina.⁴⁰ The permeation of the drug through the direct penetration pathway has been modelled as a diffusion process and studied using Fick's second law of diffusion in conjunction with an effective diffusivity for the porous media. Using the developed model, the transient mean plasma concentration \bar{C} of the drug anecortave desacetate in the choroid has been predicted. The effect of choroidal blood flow on the transient peak mean plasma concentration \bar{C}_{\max} has been studied and compared with available experiments.⁴¹ In the computational domain, the sclera and the choroid have been treated as homogeneous isotropic porous media.

The conservation equations for porous media have been solved to obtain the concentration distribution within the domain. The volume averaged momentum and species transport equations for porous media in the sclera and the choroid are written as,

$$\phi_s \frac{\partial C}{\partial t} = D_s \nabla^2 C, \quad (8)$$

$$\phi_c \frac{\partial C}{\partial t} + (\mathbf{v}_b \cdot \nabla) C = D_c \nabla^2 C, \quad (9)$$

$$\rho_b \left[\frac{\partial \mathbf{v}_b}{\partial t} + (\mathbf{v}_b \cdot \nabla) \mathbf{v}_b \right] = -\nabla P + \mu_b \nabla^2 \mathbf{v}_b - \frac{\phi_c \mu_b}{K_c} \mathbf{v}_b. \quad (10)$$

The conservation equations have been numerically solved employing the Finite Volume Method (FVM). The position and time dependent concentrations of the drug in the sclera and the choroid have been predicted and the relative magnitudes of the periocular, vitreous and circulation losses have been compared for various blood flow velocities. The simulations also predicted the transient mean plasma concentration of the drug anecortave desacetate in the choroid and the effect of choroidal blood flow on the peak mean plasma concentration.

Transdermal drug delivery is being increasingly used to deliver small, low dosage drugs through the skin as patches. Second generation transdermal drug delivery systems use physical and chemical enhancers to improve drug permeation through the skin. Low-frequency ultrasound has been used as transdermal drug delivery enhancer. Tezel and coworkers used a modified porous pathway model to achieve a detailed understanding of the pathways responsible for hydrophilic permeant delivery under ultrasound. The results of this study showed that low-frequency sonophoresis creates pathways for permeant delivery with a wide range of pore sizes.⁴²

Microneedle assisted drug delivery has been developed in recent years as a third generation transdermal drug delivery technique. Lv and coworkers have recently developed quantitative theoretical models based on porous media to simultaneously characterize the flow and drug transport.⁴³ Numerical solutions were performed to predict the kinetics of dispersed drugs injected into the skin from a microneedle array. Increasing the initial injection velocity and accelerating the blood circulation in skin tissue with high porosity were found to enhance the transdermal drug delivery.

Another emerging transdermal drug delivery technique is skin electroporation where the skin is exposed to a series of electric pulses, resulting in the structural alteration of the *stratum corneum*. Becker recently reviewed the current understanding of porous media descriptions of nondestructive transdermal transport and models of electroporation related structural changes within the skin.⁴⁴ Becker also showed the applicability and potential of merging transdermal transport modeling with skin electroporation modeling, by developing an example model that combines a brick and mortar style skin representation with a thermodynamic based model of skin electroporation.

3.4. Drug Eluting Stents

Endovascular drug-eluting stents are being increasingly used for the prevention and cure of

restenosis. Stents are devices inserted into arteries to widen their lumen, prevent occlusion and restore blood flow perfusion to the tissues downstream. Drug eluting stents combine mechanical support of restricted lumen with local drug delivery. In these stents, the therapeutic agent is loaded into biocompatible polymeric layers that are coated on the metallic struts of the stent. The release of the drug depends on many factors, such as the coating geometry and physico chemical properties, and drug characteristic, such as diffusivity and solubility. These stents work under complex stress conditions that vary in time and it is difficult to accurately predict their performance and efficiency over extended periods of time.⁴⁵

There have been a few computational approaches to understand the mass transport in drug eluting stents. The arterial wall can be seen as an inter-channelled porous medium where free drug molecules, moving in the channels, progressively bind to proteins and are metabolised. Thus, many of these approaches model the arterial wall as a homogenous porous medium, including drug advection due to the plasma filtration through the tissue. An early one-dimensional porous medium model by Lovich and Edelman showed that when the arteries were uniformly loaded with heparin, most of the drug was cleared in less than one hour, illustrating the need for sustained modes of delivery.⁴⁶

Seo and Barakat studied the influence of various Reynolds numbers, drug diffusivities and stent diameters on drug deposition to design stents with minimum flow disturbance.⁴⁷ Migliavacca and coworkers developed numerical models based on finite element method including the presence of the atherosclerotic plaque, the artery and the coronary stent.⁴⁸ The heterogeneous arterial wall was mathematically treated on a macroscopic scale as a homogeneous porous medium and the transport of the drug molecules was modelled by the macroscopic convection diffusion equation. These models considered mechanical effects of the stent expansion as well as the effect of drug transport from the expanded stent into the arterial wall. Results enabled quantification of stress field in the vascular wall, the tissue prolapse within the stent struts, as well as the drug concentration at any location and time inside the arterial wall, together with several related quantities such as drug dose and residence times.

Pontrelli and coworkers developed a mathematical model for the diffusion transport of a drug between two porous homogeneous media of different properties and dimensions.⁴⁵ The work simulated and predicted the dynamics of

a drug through a two-layered medium to estimate the dose absorption rate. The mathematical formulation was able to incorporate the drug consumption effect due to tissue cell binding. In a later study, Pontrelli developed a four layer model to analytically solve the transient drug diffusion problem in adjoining porous wall layers faced with a drug-eluting stent.⁴⁹ Even though the blood flow was not coupled to the system, the simulations could estimate the local concentration and offer an easy tool for computing the residence time of a drug.

Kolachalama et al.⁵⁰ employed computational fluid dynamic modeling to investigate the influence of luminal flow patterns on arterial drug deposition and distribution, assuming the arterial wall to be a porous medium. It was shown that the disparity in sizes of the two recirculation zones and the asymmetry in drug distribution are determined by a complex interplay of local flow and strut geometry.

Vairo and co-workers reported a multiscale and multidomain advection-diffusion model to describe drug dynamics in the polymeric substrate covering the stent, into the arterial wall, and in the vessel lumen.⁵¹ The model accounted for tissue microstructure (anisotropic drug diffusion, porosity, drug retention induced by resident proteins), macrostructure (plaque between stent and tissue), and local hemodynamics. The strut cross-section, embedment level and disturbance effects to the local blood flow were found to affect the amount of drug in the wall. Drug release was also strongly affected by the coating properties. Drug levels were strongly affected by the presence of a plaque between stent and tissue.

3.5. Functions of Organs as Flow Through Porous Medium

Porous medium modelling has been applied not only at the tissue level, but also at the organ level. For example, the lung, under SEM investigation appears like a sponge with anatomic complexity including multiple bifurcations and microscopic cavities making it a classic porous medium. The airflow and gas exchanges within a lung may be considered examples of fluid flow through porous medium. The fact that the lung has a finite boundary condition dictated by the visceral pleura makes it an ideal case for numerical simulations using porous medium models.

In the late 1990s, Koulisch (Kulich) and co-workers developed a mathematical model based on the volume-averaging technique to simulate the diffusion process within the alveolar region of the lung. The steady-state solution of the macroscopic

model was used to obtain the lung effective diffusivity, with known lung diffusing capacity.⁵² They later developed a macroscopic gas transport model to simulate the three-dimensional, unsteady respiration process within the alveolar region of the lungs. The simulations mimicked the single-breath technique for measuring the lung diffusing capacity for carbon-monoxide (CO) and predicted effect of red blood cell (RBC) distribution on the lung diffusing capacity.⁵³

Lewis and Owen used the homogenization theory to predict the macroscopic behaviour of lung tissue based upon the three dimensional microstructure of respiratory regions, making the simplifying assumption that the microstructure is periodic.⁵⁴ Equations for macroscopic air flow, pressure, and tissue deformation were formulated with parameters determined from a specification of the tissue microstructure and its material properties. The dependence of lung tissue shear viscosity on the frequency of forcing, known as the structural damping hypothesis was proposed.

Lande and co-workers modelled the lung as a viscoelastic porous medium to characterise the dynamics of gas flow.⁵⁵ The lung input impedance was considered on a macro level and parenchymal tissue impedance on the level of an alveolar wall. This lung impedance incorporated parameters of porosity, permeability, and viscoelasticity on micro and macro levels of parenchymal tissue. The macroscopic tissue deformations were represented by the linearised Navier—Stokes equations. Their study showed the impact of loading impedance at the lung boundary on the dynamic behaviour of whole lung viscoelasticity.

Kuwahara et al. proposed a porous medium approach to investigate the characteristics of the bifurcating airflow and mass transfer within a lung.⁵⁶ A two-medium treatment for the air convection and the diffusion in its surrounding wall tissue was used and the oxygen mass transfer between the inhaling air and the tissue was considered along with the effects of the blood perfusion on the mass transfer within the tissue. The analysis justified the need for 23 bifurcation levels that are found in the human respiratory to achieve minimum overall mass transfer resistance for the mass transport from the external air to the red blood cells—an observation consistent with Bejan's constructal law ("for a flow system to persist in time, it must evolve in such a way that it provides easier access to its currents").

The heart muscle, containing the intracoronary vasculature and the kidney, where the porous character is essential for the blood filtration are other organs that can be modelled as porous media.

Cunrman and Rohan presented a numerical model to describe diffusion-deformation processes in the heart muscle and the kidney.⁵⁷ The model consisted of the equilibrium equation and a number of mass conservation equations, incorporating the Darcy law of fluid diffusion. In the heart case, the model helped understand the distribution of the perfusing blood during the cardiac cycle. In the case of kidneys, the model aimed at simulating extreme dynamical loads on the kidney during the car accidents.

There have been reports of modeling hemodialysers (“artificial kidneys”) as porous medium. Liao and coworkers developed a porous medium model to simulate mass transfer in artificial kidney. Darcy’s equations were employed to simulate shell-side flow, Navier Stokes equations were employed to simulate lumen-side flow, and Kedem-Katchalsky equations were used to compute transmembrane flow.⁵⁸ Ding and coworkers have also presented a double porous media model using Navier Stokes equations with Darcy source terms and Modified Kedem Katchalsky equations for mass transfer of hollow fiber hemodialyzers.⁵⁹

Smye and coworkers developed a mathematical model of the complex permittivity of liver tissue as a function of frequency f , in the range $10^4 < f < 10^7$ Hz, derived from a formulation used to describe the complex permittivity of porous media.⁶⁰ The complex permittivity for a plausible porosity and percolation probability distribution was calculated and compared with the published measured electrical properties of liver tissue.

The brain can be considered a porous medium of a solid phase (brain tissue) and a fluid phase (interstitial fluid or blood plasma. At the end of the last century, Dai and Mura developed a lattice cellular automata model for ion diffusion within the brain-cell microenvironment and performed numerical simulations using the corresponding Lattice Boltzmann equation.⁶¹ Sen and Bassar modelled diffusion in brain white matter fascicles as a problem of diffusion in an array of identical thick-walled cylindrical tubes immersed in an outer medium and arranged periodically in a regular lattice. For an impermeable myelin sheath, diffusing molecules within the inner core were found to be completely restricted, while molecules in the outer medium were hindered due to the tortuosity of the array of impenetrable tubes.⁶²

Wagner and Ehlers used a porous medium model to obtain coupled partial differential equations that were then discretised using mixed finite elements with a backward Euler time integration. Numerical examples illustrated the fundamental effects on the brain tissue under heart-rate dependent pulsative pressure variations.⁶³

Drysdale et al. formulated a quantitative theory to relate stimulus and the resulting blood oxygen level dependent (BOLD) functional MRI signal (an indirect measure of neuron activity) through modeling of the brain as a porous elastic medium with vasculature represented by interconnected pores. The model incorporated conservation of blood mass, interconversion of oxygenated and deoxygenated hemoglobin, force balance within the blood and of blood pressure with vessel walls, and blood flow modulation due to neuronal activity.⁶⁴

Peristalsis is a major physiological mechanism for fluid transport in many biological systems. Peristaltic mechanism is involved in swallowing food via the esophagus, urine transport from kidney to bladder through ureter, fluids movement of lymphatic fluids in lymphatic vessels, flow of bile from gall bladder into the duodenum, spermatozoa in the ductus efferentes of the male reproductive tract and cervical canal, movement of ovum in the fallopian tube and circulation of blood in small blood vessels. Peristaltic transport is also employed in various biomedical applications such as the heartlung machine, blood pump machine and dialysis machine.

There have been a few studies on the numerical analysis of peristaltic fluid transport in such applications through the porous medium approach. The first study was presented by Elshehawey et al.⁶⁵ Maiti and Misra numerically studied peristaltic transport of bile in bile duct in the presence of stones as a transport through porous channel problem.⁶⁶ The effects of various parameters, such as Reynolds number, pressure gradient, porosity parameter, Darcy number, slip parameter, amplitude ratio and wave number on velocity and critical pressure for reflux were studied and results were found to agree with existing experimental and analytical data. It was further shown that bile velocity decreases as the number of stones increase and when bile contains a very large number of stones, reflux occurs when the critical pressure is quite small.

In another study, Tripathi and co-workers studied the peristaltic transport of a generalized Burgers fluid under the assumptions of long wavelength and low Reynolds number.⁶⁷ This model is applicable to study the movement of chyme in the small intestine. They concluded that the movement of viscoelastic chyme with generalized Burgers model through the small intestine is more favoured compared to the movement of viscoelastic chyme with fractional generalized Burgers model. Kothandapani and Srinivas studied non-linear peristaltic transport

of a Newtonian fluid in an inclined asymmetric channel through a porous medium to understand fluid dynamic aspects of the intra-uterine fluid flow through a porous medium.⁶⁸ The influence of several pertinent parameters on the stream function and pressure drop has been studied and numerical results obtained are presented. Rathod and Channakote studied the peristaltic transport of a viscous incompressible fluid through a porous medium using the geometrical form of the ureter.⁶⁹ The analytical expressions for the stream function, axial velocity, and pressure gradient were obtained and the effect of various parameters on the flow was discussed.

3.6. Porous Medium Models of Microbial Transport

A variety of microbes including virus and bacteria are constantly released into the subsurface as a result of human activities and other natural causes. The fate of the microbe in the porous subsurface is important in deciding the levels of contamination of land and subsurface water. Sim and Chrysikopoulos developed a numerical model for one-dimensional virus transport in homogeneous, unsaturated porous media. The model accounted for virus sorption onto liquid-solid and air-liquid interfaces as well as inactivation of viruses suspended in the liquid phase and viruses attached at both interfaces. The effects of the moisture content variation on virus transport in unsaturated porous media were investigated. Model simulations indicated that virus sorption is greater at air-liquid than liquid-solid interfaces.⁷⁰

Schijven and Simunek analysed bacteriophage removal by soil passage in two field studies to investigate differences between one- and two-dimensional modeling approaches, differences between one- and two-site kinetic sorption models, and the role of heterogeneities in the soil properties.⁷¹ The software packages HYDRUS-1D and HYDRUS-2D, which simulate water flow and solute transport in one- and two-dimensional variably saturated porous media, respectively, were used in the study. The two-site model performed better than the one-site model in describing bacteriophage concentrations for the deep well injection study.

Barth and Hill evaluated the importance of seven types of parameters to virus transport: hydraulic conductivity, porosity, dispersivity, sorption rate and distribution coefficient (representing physical-chemical filtration), and in-solution and adsorbed inactivation (representing virus inactivation).⁷² One- and two-dimensional homogeneous simulations,

designed from published field experiments, and sensitivity-analysis methods, were conducted to establish that hydraulic conductivity, porosity, and sorption are the most important parameters that affect virus-transport predictions.

Oats and coworkers developed an experimental method and numerical model to understand reactive microbial transport in saturated porous media. The advection dispersion equation was used to model bacterial transport and oxygen concentration was modelled assuming bacterial consumption via Monod kinetics with consideration of additional effects of rate-limited mass transfer from residual gas bubbles.⁷³ Sun and Wheeler formulated a primal discontinuous Galerkin (DG) method to solve the transport equations for modeling migration and survival of viruses with kinetic and equilibrium adsorption in porous media.¹⁵ Results showed that DG methods can treat bioreactive transport of viruses over a wide range of modeling parameters, including both advection- and dispersion-dominated problems. DG was also shown to be able to sharply capture local phenomena of virus transport with dynamic mesh adaptation.

Nathalie Tufenkji has reviewed traditional approaches used to model microbial transport and fate in saturated porous media.⁷⁴ The review presented the general governing equations typically considered in models of microbial transport and fate. The limitations of the mathematical models and recently proposed initiatives have also been discussed.

Bhattacharjee and coworkers developed a two-dimensional model for virus transport in physically and geochemically heterogeneous subsurface porous media.⁷⁵ The model solved the advection dispersion equation, with an additional factor of virus inactivation in the solution, as well as virus removal at the solid matrix surface due to attachment (deposition), release, and inactivation. The study reports two surface inactivation models for the fate of attached inactive viruses and their subsequent role on virus attachment and release. Geochemical heterogeneity was modelled as patches of positively charged metal oxyhydroxide coatings on collector grain surfaces. Physical heterogeneity was represented as spatial variability of hydraulic conductivity. The upstream weighted multiple cell balance method was employed to numerically solve the governing equations of groundwater flow and virus transport. Subsurface layered geochemical and physical heterogeneity was found to significantly affect virus mobility. Random distributions of physical and geochemical heterogeneity was also found to influence virus

transport behaviour. Large virus release rates resulted in extended periods of virus breakthrough over significant distances downstream from the injection sites.

Bekhitt et al. studied the combined effect of colloids and bacteria on contaminant transport through development of a conceptual model using the mass balance equation for each constituent in its different forms and by expressing the reactions among constituents and with the porous medium using a linear kinetic model.⁷⁶ The conceptual and mathematical models incorporated bacterial growth and decay, bacterial chemotaxis, bacterial lysing and contaminant utilization. Finite difference method with a third-order total variation diminishing (TVD) scheme was used to solve the model. The results were found to agree with earlier experimental observations.

Sharma and Srivastava simulated viral transport through two-dimensional heterogeneous porous media at field scale using an advective dispersive virus transport equation with first-order adsorption and inactivation constant.⁷⁷ Implicit finite-difference numerical technique was used to solve the two-dimensional virus transport equation for virus concentration in suspension. Higher values of mass transfer rate constant and inactivation constant lead to reduced virus concentration and increase in the variance of conductivity field or its correlation length resulted in a higher virus concentration.

4. Porous Medium Modeling in Bio-Heat Transport

Living tissues are complex structures and the heat transfer in them involves primarily heat conduction in tissue, convection heat transfer between blood and vessel, and blood perfusion, which cannot be understood using simplistic models. The living tissue ensemble can however be conceived as a fluid saturated porous medium including the effects of blood perfusion to help understand their heat transfer. A generic region of biological tissue irrigated by blood flow can readily be perceived to fit our definition of a porous medium comprising a stationary solid (tissue) matrix saturated by fluid (blood) flow, with identifiable interfaces at a resolution level. The heat transport in such biological tissue region can be modelled as convection in porous media with internal heat generation.⁷⁸

From this perspective, it is apparent that the investigation of heat transfer processes in such a tissue-blood region would require an energy conservation statement similar to the porous medium energy conservation equation, Eq. (7),

discussed earlier. A heat transfer equation similar in purport was proposed by Chen and Holmes in 1980, although, without the claim of being a porous medium model.

Chen and Holmes divided the control volume occupied by the tissue and blood vessels into two separate volumes: one consisting of solid tissue only, and the other of blood in the vascular space within the blood vessels.⁷⁹ While the term “porous medium” was not explicitly used in this work, such a division of the system into the stationary tissue phase and the fluid blood phase fits our definition of a classic porous medium with identifiable interfaces. The proposed ‘continuum model’ assumes that heat transfer between blood and surrounding tissue occurs along the circulatory network after the blood flows through the terminal arteries and before the arterioles and that there is no significant heat transfer between tissue and blood within the capillary region until the blood reaches the terminal veins. The Chen and Holmes model can be written as

$$(\rho c)_e \frac{\partial T_e}{\partial t} = k_e \nabla^2 T_e + k_p \nabla^2 T_e + V_j^m (\rho c_p)_b (T_a - T_e) - (\rho c_p)_b \vec{v} \cdot \nabla T_e + Q_m''' \quad (11)$$

Here, k_p is the perfusion conductivity. The first two terms on the RHS of the equation are the effective heat conduction and apparent conductive heat transfer enhancement due to blood flow respectively. The $V_j^m (\rho c_p)_b (T_a - T_e)$ is the local blood perfusion term at the j -th branching level of blood vessel. $(\rho c_p)_b \vec{v} \cdot \nabla T_e$ is the convection transport term to account for the effect of blood flow direction within tissue and Q_m''' is the volumetric metabolic heat generation.

The averaging of the temperature ($T_e = f(T_t, T_b)$ where T_t and T_b are tissue and blood temperatures) and related thermo-physical properties of tissue and blood (k and c) carried out when writing Eq. (11) is much similar to the volume averaging procedure discussed in Section 2. However, the models used for k_e and c_e is *ad hoc* and not based on any assumed local porous structure for the biological tissue region. Hence, Eq. (11) is defined not on a REV based porous continuum like Eq. (7), the porous medium energy balance, even when local thermal equilibrium exist between tissue and blood.

Neglecting the local (point-wise) effects of blood flow (dispersion or perfusion conductivity effect), the thermo-physical properties take values for the tissue and setting $T_e = T_t$, the Chen and Holmes model, Eq. (11), can be reduced to the Pennes bio-heat transfer equation, the earliest and

rudimentary bio-heat model that first accounted for the blood perfusion effect,⁸⁰ as

$$(\rho c)_t \frac{\partial T_t}{\partial t} = -k_t \nabla^2 T_t + Q_m'' + (\omega \rho c_p)_b (T_a - T_t) \quad (12)$$

where ω is the Pennes blood perfusion rate, a global quantity used ad hoc inside the differential bio-heat equation. The T_a is the arterial temperature dependent on human anatomy (Pennes used it for human forearm, where he had experimental data). The Pennes bio-heat transfer equation is commonly used to model energy transport in biological systems. Although the Pennes bioheat equation recognizes the different temperatures between the tissues and blood, the blood temperature is assumed to be a constant throughout the heat transfer domain. Also, it is not based on the porous medium approach.

A logical extension of the Chen and Holmes model is a two-energy heat transfer model with a connecting interphase heat transfer relationship. Such a model has been derived from first principles by Nakayama and Kuwahara.⁸¹ The individual macroscopic energy equations were written for the blood and tissue phases as follows

For blood phase:

$$\begin{aligned} \epsilon \rho_f c_{pf} \frac{\partial \langle T \rangle^f}{\partial t} + \rho_f c_{pf} \frac{\partial}{\partial x_j} \langle u_j \rangle \langle T \rangle^f \\ = \frac{\partial}{\partial x_j} \left(\epsilon k_f \frac{\partial \langle T \rangle^f}{\partial x_j} + \epsilon k_{disjk} \frac{\partial \langle T \rangle^f}{\partial x_k} \right) \\ - a_f h_f (\langle T \rangle^f - \langle T \rangle^s) - \rho_f c_{pf} \omega (\langle T \rangle^f - \langle T \rangle^s) \end{aligned} \quad (13)$$

In the above equation, the LHS is the macroscopic convection term, while the four terms on the RHS correspond to the macroscopic conduction, thermal dispersion, interfacial convective heat transfer and blood perfusion, respectively.

For the tissue phase:

$$\begin{aligned} (1 - \epsilon) \rho_s c_s \frac{\partial \langle T \rangle^s}{\partial t} = \frac{\partial}{\partial x_j} \left((1 - \epsilon) k_s \frac{\partial \langle T \rangle^s}{\partial x_j} \right) \\ + a_f h_f (\langle T \rangle^f - \langle T \rangle^s) \\ + \rho_f c_{pf} \omega (\langle T \rangle^f - \langle T \rangle^s) \\ + (1 - \epsilon) S_m \end{aligned} \quad (14)$$

In Eqs. (13) & (14), the angle brackets signify average quantities and the average is taken over either solid (tissue) or fluid (blood) volume at the REV level (see Fig. 1). In the tissue, the LHS represents the thermal inertia term, and the terms on the right hand-side correspond to the macroscopic conduction, interfacial convective

heat transfer, blood perfusion heat source and metabolic heat source, respectively.

Combining the energy equation for the tissue phase with the blood and assuming local thermal equilibrium to hold between tissue and blood at the REV level, one could arrive at the porous medium form of the bio-heat equation, which would resemble the Chen and Holmes model in Eq. (11) without the global blood perfusion term and the perfusion or dispersion conductivity term.

Nield and Kuznetsov proposed an illustrative model for bio-heat transfer and provided an analytical solution for forced convection in a parallel plate channel occupied by a layered saturated porous medium with counterflow, the dominant feature that distinguishes bio-heat transfer from other forms of heat transfer.⁸² The case of asymmetrical constant heat-flux boundary conditions is considered and the Brinkman model was employed for the porous medium.

Belmiloudi studied the effects blood perfusion rate and the porosity parameters on the transient temperature of biological tissues for use in thermal diagnostics applications such as laser surgery and thermotherapy often used in the treatment of cancer.⁸³ A generalized transient bioheat transfer type model has been introduced and the existence, the uniqueness and the regularity of the solution of the state equation are established.

Fourier's heat conduction model has been found to be sufficient for most engineering applications. However it is insufficient for accurately predicting temperature distribution in non-homogenous materials like meat.⁸⁴ Since the human biological tissue also has a structure which is similar to porcine tissue, the study of non-Fourier energy transport in human tissues is important. An example of such an application would be laser irradiation of the retina where a high heat flux is typically applied for a short period of time. The constitutive relation between heat flux and temperature gradient, to account for a finite heat propagation velocity, was proposed by Cattaneo.⁸⁵ It states that there is a time lag τ_q between the heat flux and temperature gradient i.e. a temperature gradient ∇T at time t causes a heat flux $-k\nabla T$ to flow at time $t + \tau_q$. It was later extended to include a time lag τ_r also for the temperature gradient. Such a model is known as the dual phase lag constitutive relation between heat flux and temperature gradient.

$$q + \tau_q \frac{\partial q}{\partial t} = -k\nabla T - k\tau_r \frac{\partial(\nabla T)}{\partial t} \quad (15)$$

Retinal laser irradiation has been analysed using the bio-heat dual phase lag model for heat

conduction.⁸⁶ Both one- and three-dimensional models of the human eye was used to simulate retinal eye surgery. The laser heating was modelled as a volumetric heat source and the respective magnitudes calculated based on the absorptivities of the various layers. The retinal pigmented epithelium (RPE) is a highly pigmented layer of about 10 μm thickness where bulk of the heat absorption takes place. The sclera, choroid and the RPE were modelled as a porous medium, with the choroidal blood flow modelled as Darcy flow, Eq. (2). Numerical simulations were performed to compare temperature distributions obtained from the dual phase lag model with corresponding results from an earlier Fourier model in.⁸⁷

Based on a non-equilibrium heat transfer model in the living tissue obtained by performing volume average to the local instantaneous energy equations for blood and tissues, Zhang obtained the dual-phase lag bioheat equations with blood or tissue temperature as sole unknown temperature by eliminating the tissue or blood temperature from the non-equilibrium model.⁷⁸ In this model, the phase lag times were expressed in terms of the properties of blood and tissue and the interphase convective heat transfer coefficient and blood perfusion rate. It was found that the phase lag times for heat flux and temperature gradient for the living tissue are very close to each other.

Kou et al. studied the effects of directional blood flow and heating schemes on temperature distribution during thermal therapy of a tumour tissue using a transient bioheat transfer equation based on the porous medium property to encompass the directional effect of blood flow.⁸⁸ A Green's function was used to obtain the temperature distribution for this modified bioheat transfer equation, and the thermal dose equivalence was used to evaluate the heating results for a set of given parameters. It was found that during rapid heating, the domain of thermal lesion can effectively cover the target region. However, the region of thermal lesion may extend to the downstream normal tissue if the porosity is high ($\phi > 0.7$) and the averaged blood velocity has a larger value.

He et al. developed a finite element (FE) model to analyse the blood perfusion and heat transport in the human finger based on the transport theory in porous media.⁸⁹ The systemic blood circulation in the upper limb was modelled based on the one-dimensional flow in an elastic tube. The realistic geometric model for the human finger was constructed based on the MRI image data. After computing the capillary pressure and blood velocity in the tissue, the temperatures in

the large vessels and the tissue of the finger were computed by numerically solving the energy equation in porous media. The computed blood flow in tissues was found to be in agreement with experimental measurements.

Yuan developed an equivalent heat transfer coefficient between tissue and blood in a porous model and applied it to the thermal analysis of a biological tissue in a hyperthermia therapy.⁹⁰ A finite difference method was employed to solve the tissue temperature distribution using Pennes bio-heat transfer equation and a two-equation porous model, respectively, and then a conjugate gradient method was used to estimate the equivalent heat transfer coefficient in the two-equation porous model with a known perfusion rate in Pennes bio-heat transfer equation. The equivalent heat transfer coefficient was found not to be a strong function of the perfusion rate, blood velocity and heating conditions, but inversely relate to the blood vessel diameter.

Mahjoob and Vafai used local thermal non-equilibrium model in porous media theory to establish exact solutions for blood and tissue phase temperature profiles and overall heat exchange correlations for two primary tissue/organ models representing isolated and uniform temperature conditions. The model incorporated pertinent effective parameters, such as volume fraction of the vascular space, ratio of the blood and the tissue matrix thermal conductivities, interfacial blood-tissue heat exchange, tissue/organ depth, arterial flow rate and temperature, body core temperature, imposed hyperthermia heat flux, metabolic heat generation, and blood physical properties.⁹¹

5. Concluding Remarks

An introduction to porous medium concepts used in modelling biological fluid flow, heat and mass transfer has been presented. Research literature published after ~2002 pertaining to porous medium modelling of bio-fluid-thermal processes has also been discussed in detail. One can observe that the field of biology has become interdisciplinary with a surge of physical and mathematical concepts being invoked to model biological processes that occur at several scales.

Advancements in biology, health and medicine should inevitably require further simplified cost-effective engineering understanding of the associated biological processes. Porous medium modelling of bio-fluid and heat flows would certainly participate. For it to contribute further, detailed characterization of internal geometries of biological organs using tomographical studies at

various length scales is a prerequisite for mapping biological regions as porous medium with known porosities and permeabilities. Available conceptual ramifications like chemically reactive, deforming and bi- and tri-disperse porous media are yet to be thoroughly utilized in attempting to model suitable biological phenomena. Biological flows where the porous medium convective momentum transport terms are dominating are yet to be investigated in detail. In this sense, one could observe that the entire gamut of fluid flow types governed by the generalized porous medium momentum conservation statement is yet to be explored. Similarly, the potential of the more advanced bio-heat transfer models formulated using porous medium concepts of local thermal non-equilibrium between the tissue and blood flow, are yet to be fully realized.

While seeking simplifications for biological processes through porous medium models is an exciting and useful multidisciplinary pursuit, a note of caution is also in order. As Francis Crick, one of the giants of biology having moved to it

from physics, learned (to quote from),⁹² “you have to adjust from the elegance and deep simplicity of physics to the elaborate chemical mechanisms that natural selection has evolved over billions of years.” A related point recently⁹³ made by Walter Gratzer is worth mentioning: “physicists, along with chemists and engineers, are surging into biology. This has rejuvenated both the biological and the physical sciences, even if the leading physics journals now publish a profusion of poorly refereed papers whose authors have not followed the excellent precept not to think what one wants to think until one knows what one ought to know.” Biology is primarily governed not by fundamental physical laws—few and rigid—but by an evolutionary process of adaptation (as implied by Bio, which means life). Seeking modelling simplifications from physical principles for such complex and myriad processes could often result in incremental progress – with particular solutions of limited range of utility or general solutions to approximations that has oversimplified biological reality.

Glossary

Alveolar sac	an air sac at the terminal cavities of lung tissue to hold air.
Arterial plaque	a buildup of white blood cell (sometimes termed fatty, despite absence of adipocytes) deposits within the wall of an artery.
Artery	an elastic blood vessel that transports blood away from the heart.
Atherosclerotic plaque	accumulation of fatty material along the walls of arteries.
Bacteriophage	A virus that infects bacteria.
Blood perfusion	Delivery of arterial blood to a capillary bed in the biological tissue.
Choroid	the middle, blood vessel rich, layer of the eye, between the sclera and the retina.
Contois cell-growth model	$u = u_m \times s/(K \times x + s)$ where x is the cell concentration, s is the limiting substrate concentration, and u is the specific growth rate.
Fascicle	A bundle or cluster.
Form Coefficient	C, m^{-1} , is the summation of the form drag, originating from the local shape of the solid matrix, imposed on the fluid flow through the pores of a porous medium.
HDL	High density lipoprotein: Big-sized molecules that enable transport of lipids like cholesterol and triglycerides within the water-based bloodstream. Commonly referred to as “good cholesterol”.
Hemodialyser	an external machine that remove impurities and waste products from the bloodstream before returning the blood to the patient’s body.
Hemoglobin	An iron-containing blood protein that transports oxygen from the lungs to the tissues of the body and carries carbon dioxide from the tissues to the lungs.
Iliac	Of the upper pelvic (hip) bone.
Intima	innermost membrane of an organ or part.

LDL	Low density lipoprotein: Small-sized molecules that enable transport of lipids like cholesterol and triglycerides within the water-based bloodstream. Commonly referred to as "bad cholesterol".
LTE	Local Thermal Equilibrium; an ideal situation, when assumed to exist locally, negates interfacial heat transfer between the solid and fluid constituent of a porous medium.
LTNE	Local Thermal Non-Equilibrium; is the actual situation that exists locally permitting interfacial heat transfer between the solid and fluid constituent of a porous medium. Since this implies the solid and fluid to have different temperatures even in steady state, an interfacial heat transfer coefficient is required for closure of the energy conservation equation.
Myelin sheath	The insulating envelope that surrounds the core of a nerve fiber to transmit nerve impulses.
Parenchyma	the functional tissue of an organ.
Peristalsis	wavelike muscular contractions of tubular structures.
Permeability	K, m^2 , hydraulic property of a porous medium that is a summation of the viscous drag offered by the solid matrix to the flow through the pores.
Porosity	or Volumetric Porosity is the ratio of the pore volume to the total volume of a porous medium. In general, a direction dependent surface porosity, using the ratio of the respective areas, can also be defined for a porous medium.
RPE	retinal pigmented epithelium: The pigmented layer of the retina.
Sclera	The tough, opaque, usually white, fibrous outer envelope of the eye covering all of the eyeball except the cornea; Commonly referred to as the white of the eye.
Stratum corneum	outer skin layer consisting of dead cells.
Transdermal	Across the skin.
Transmural flow	Flow through the wall of an organ.
Transcleral flow	Flow through Sclera, sheathing the eye.

Received date TK

References

1. C. K. Charny, *Mathematical Models of Bioheat Transfer*, Chapter 2, Academic Press Inc., Boston, USA., 1992, Ch. *Advances in Heat Transfer*, pp.19–156.
2. A.-R. Khaled, K. Vafai, The role of porous media in modeling flow and heat transfer in biological tissues, *International Journal of Heat and Mass Transfer* 46 (26) (2003) 4989–5003. doi:10.1016/S0017-9310(03)00301-6.
3. C. Nicholson, Diffusion and related transport mechanisms in brain tissue, *Reports on Progress in Physics* 64 (7) (2001) 815. URL <http://stacks.iop.org/0034-4885/64/i=7/a=202>.
4. K. Khanafer, K. Vafai, The role of porous media in biomedical engineering as related to magnetic resonance imaging and drug delivery, *Heat and Mass Transfer* 42 (2006) 939–953, 10.1007/s00231-006-0142-6. URL <http://dx.doi.org/10.1007/s00231-006-0142-6>.
5. J. Lage, *The Fundamental Theory of Flow through Permeable Media: from Darcy to Turbulence*, Pergamon, New York, 1988, Ch. *Transport Phenomena in Porous Media*, pp. 1–30.
6. D. A. Nield, A. Bejan, *Convection in Porous Media*, 3rd ed., Springer-Verlag, New York., 2006.
7. N. Yang, K. Vafai, Modeling of low-density lipoprotein (Ldl) transport in the artery – effects of hypertension, *International Journal of Heat and Mass Transfer* 49 (5–6) (2006) 850–867. doi:10.1016/j.ijheatmasstransfer.2005.09.019.
8. Wikipedia, Atheroma, Online (Public Domain Image) (2011). URL <http://en.wikipedia.org/wiki/Atheroma>.
9. M. Prosi, P. Zunino, K. Perktold, A. Quarteroni, Mathematical and numerical models for transfer of low-density lipoproteins through the arterial walls: a new methodology for the model set up with applications to the study of disturbed luminal flow, *Journal of Biomechanics* 38 (4) (2005) 903–917. doi:10.1016/j.jbiomech.2004.04.024.
10. G. Karner, K. Perktold, Effect of endothelial injury and increased blood pressure on albumin accumulation in the arterial wall: a numerical study, *Journal of Biomechanics* 33 (6) (2000) 709–715. doi:10.1016/S0021-9290(99)00226-2.
11. N. Sun, N. Wood, A. Hughes, S. Thom, X. Xu, Fluid-wall modelling of mass transfer in an axisymmetric stenosis: Effects of shear-dependent transport properties, *Annals of Biomedical Engineering* 34 (2006) 1119–1128, 10.1007/s10439-006-9144-2. doi:10.1007/s10439-006-9144-2.
12. U. Olgac, D. Poulidakos, S. C. Saur, H. Alkadhi, V. Kurtcuoglu, Patient-specific three-dimensional simulation of Ldl accumulation in a human left coronary artery in its healthy and atherosclerotic states, *American Journal of Physiology—Heart and Circulatory Physiology* 296 (6) (2009) H1969–H1982. arXiv:<http://ajpheart.physiology.org/content/296/6/H1969.full.pdf+html>, doi:10.1152/ajpheart.01182.2008.

13. S. Tada, J. M. Tarbell, Internal elastic lamina affects the distribution of macromolecules in the arterial wall: a computational study, *American Journal of Physiology—Heart and Circulatory Physiology* 287 (2) (2004) H905–H913. arXiv:<http://ajpheart.physiology.org/content/287/2/H905.full.pdf+html>, doi:10.1152/ajpheart.00647.2003.
14. N. Sun, N. B. Wood, A. D. Hughes, S. A. M. Thom, X. Yun Xu, Effects of transmural pressure and wall shear stress on ldl accumulation in the arterial wall: a numerical study using a multilayered model, *American Journal of Physiology—Heart and Circulatory Physiology* 292 (6) (2007) H3148–H3157. arXiv:<http://ajpheart.physiology.org/content/292/6/H3148.full.pdf+html>, doi:10.1152/ajpheart.01281.2006.
15. S. Sun, M. F. Wheeler, Discontinuous galerkin methods for simulating bioactive transport of viruses in porous media, *Advances in Water Resources* 30 (6–7) (2007) 1696–1710, biological processes in porous media: From the pore scale to the field. doi:10.1016/j.advwatres.2006.05.033.
16. L. Ai, K. Vafai, A coupling model for macromolecule transport in a stenosed arterial wall, *International Journal of Heat and Mass Transfer* 49 (9–10) (2006) 1568–1591. doi:10.1016/j.ijheatmasstransfer.2005.10.041.
17. M. Khakpour, K. Vafai, Critical assessment of arterial transport models, *International Journal of Heat and Mass Transfer* 51 (3–4) (2008) 807–822. doi:10.1016/j.ijheatmasstransfer.2007.04.021.
18. M. Khakpour, K. Vafai, Effects of gender-related geometrical characteristics of aorta-iliac bifurcation on hemodynamics and macromolecule concentration distribution, *International Journal of Heat and Mass Transfer* 51 (23–24) (2008) 5542–5551, biomedical-Related Special Issue. doi: 10.1016/j.ijheatmasstransfer.2008.04.025.
19. N. Koshiba, J. Ando, X. Chen, T. Hisada, Multiphysics simulation of blood flow and ldl transport in a porohyperelastic arterial wall model, *Journal of Biomechanical Engineering* 129 (3) (2007) 374–385. doi:10.1115/1.2720914.
20. S. Badia, A. Quaini, A. Quarteroni, Coupling biot and navier-stokes equations for modelling fluid-poroelastic media interaction, *Journal of Computational Physics* 228 (21) (2009) 7986–8014. doi:10.1016/j.jcp.2009.07.019.
21. J. A. Cooper, H. H. Lu, F. K. Ko, J. W. Freeman, C. T. Laurencin, Fiber-based tissue-engineered scaffold for ligament replacement: design considerations and in vitro evaluation, *Biomaterials* 26 (13) (2005) 1523–1532. doi:10.1016/j.biomaterials.2004.05.014.
22. Wikipedia, Tissue engineering, Online (Public Domain Image) (2011). URL <http://en.wikipedia.org/wiki/Tissueengineering>.
23. D. Lasseux, A. Ahmadi, X. Cleis, J. Garnier, A macroscopic model for species transport during in vitro tissue growth obtained by the volume averaging method, *Chemical Engineering Science* 59 (10) (2004) 1949–1964. doi:10.1016/j.ces.2004.02.003.
24. B. Porter, R. Zael, H. Stockman, R. Guldborg, D. Fyhrie, 3-d computational modeling of media flow through scaffolds in a perfusion bioreactor, *Journal of Biomechanics* 38 (3) (2005) 543–549. doi:10.1016/j.jbiomech.2004.04.011.
25. V. A. F. Costa, L. A. Oliveira, B. R. Baliga, A. C. M. Sousa, Simulation of coupled flows in adjacent porous and open domains using a control-volume-finite-element-method, *Numerical Heat Transfer Part A-applications* 45 (2004) 675–697. doi:10.1080/10407780490424839.
26. L. Betchen, A. Straatman, B. Thompson, A nonequilibrium finite-volume model for conjugate fluid/porous/solid domains, *Numerical Heat Transfer Part A—Applications* 49 (2006) 543–565. doi:10.1080/10407780500430967.
27. F. Boschetti, M. T. Raimondi, F. Migliavacca, G. Dubini, Prediction of the micro-fluid dynamic environment imposed to three-dimensional engineered cell systems in bioreactors, *Journal of Biomechanics* 39 (3) (2006) 418–425. doi:10.1016/j.jbiomech.2004.12.022.
28. T. Adachi, Y. Osako, M. Tanaka, M. Hojo, S. J. Hollister, Framework for optimal design of porous scaffold microstructure by computational simulation of bone regeneration, *Biomaterials* 27 (21) (2006) 3964–3972. doi:10.1016/j.biomaterials.2006.02.039.
29. F. Coletti, S. Macchietto, N. Elvassore, Mathematical modeling of three-dimensional cell cultures in perfusion bioreactors, *Industrial & Engineering Chemistry Research* 45 (24) (2006) 8158–8169. arXiv:<http://pubs.acs.org/doi/pdf/10.1021/ie051144v>, doi:10.1021/ie051144v.
30. C. Chung, C. Chen, C. Chen, C. Tseng, Enhancement of cell growth in tissue-engineering constructs under direct perfusion: Modeling and simulation, *Biotechnology and Bioengineering* 97 (6) (2007) 1603–1616. doi:10.1002/bit.21378.
31. J. Sanz-Herrera, J. Garca-Aznar, M. Doblar, Micro-macro numerical modelling of bone regeneration in tissue engineering, *Computer Methods in Applied Mechanics and Engineering* 197 (33–40) (2008) 3092–3107. doi: 10.1016/j.cma.2008.02.010.
32. P. Yu, T. S. Lee, Y. Zeng, H. T. Low, Fluid dynamics and oxygen transport in a micro-bioreactor with a tissue engineering scaffold, *International Journal of Heat and Mass Transfer* 52 (1–2) (2009) 316–327. doi:10.1016/j.ijheatmasstransfer.2008.06.021.
33. R. J. Whittaker, R. Booth, R. Dyson, C. Bailey, L. P. Chini, S. Naire, S. Payvandi, Z. Rong, H. Woollard, L. J. Cummings, S. L. Waters, L. Mawasse, J. B. Chaudhuri, M. J. Ellis, V. Michael, N. J. Kuiper, S. Cart-mell, Mathematical modelling of fibre-enhanced perfusion inside a tissue-engineering bioreactor, *Journal of Theoretical Biology* 256 (4) (2009) 533–546. doi:10.1016/j.jtbi.2008.10.013.
34. D. Y. Arifin, L. Y. Lee, C.-H. Wang, Mathematical modeling and simulation of drug release from microspheres: Implications to drug delivery systems, *Advanced Drug Delivery Reviews* 58 (12–13) (2006) 1274–1325, computational Drug Delivery. doi:10.1016/j.addr.2006.09.007.
35. T. W.-Y. Lee, J. R. Robinson, Drug delivery to the posterior segment of the eye ii: development and validation of a simple pharmacokinetic model for subconjunctival injection, *Journal of Ocular Pharmacology and Therapeutics* 20 (1) (2004) 43–53. doi:10.1089/108076804772745455.
36. T. W.-Y. Lee, J. R. Robinson, Drug delivery to the posterior segment of the eye iii: the effect of parallel elimination pathway on the vitreous drug level after subconjunctival injection, *Journal of Ocular Pharmacology and Therapeutics* 20 (1) (2004) 55–64. doi:10.1089/108076804772745464.
37. H. Kim, M. R. Robinson, M. J. Lizak, G. Tansey, R. J. Lutz, P. Yuan, N. S. Wang, K. G. Csaky, Controlled drug release from an ocular implant: an evaluation using dynamic three-dimensional magnetic resonance imaging., *Investigative Ophthalmology & Visual Science* 45 (8) (2004) 2722–31. doi: 10.1167/iovs.04-0091.
38. V.-P. Ranta, A. Urtili, Transscleral drug delivery to the posterior eye: Prospects of pharmacokinetic modeling, *Advanced Drug Delivery Reviews* 58 (2006) 1164–1181. doi:10.1016/j.addr.2006.07.025.

39. R. K. Balachandran, V. H. Barocas, Computer modeling of drug delivery to the posterior eye: Effect of active transport and loss to choroidal blood flow, *Pharmaceutical Research* 25 (11) (2008) 2685–2696.
40. A. Narasimhan, V. Ramanathan, Effect of choroidal blood flow on trans-cleral retinal drug delivery using a porous medium model, *International Journal of Heat and Mass Transfer* (2011) Under Review.
41. D. C. Dahlin, M. H. Rahimy, Pharmacokinetics and metabolism of anecor-tave acetate in animals and humans, *Survey of Ophthalmology* 52 (1) (2007) S49–S61. doi:10.1016/j.survophthal.2006.11.002.
42. A. Tezel, A. Sens, S. Mitragotri, Description of transdermal transport of hydrophilic solutes during low-frequency sonophoresis based on a modified porous pathway model, *Journal of Pharmaceutical Sciences* 92 (2) (2003) 381–393. doi:10.1002/jps.10299.
43. Y.-G. Lv, J. Liu, Y.-H. Gao, B. Xu, Modeling of transdermal drug delivery with a microneedle array, *Journal of Micromechanics and Microengineering* 16 (11) (2006) 2492. URL <http://stacks.iop.org/0960-1317/16/i=11/a=034>.
44. S. M. Becker, Skin electroporation with passive transdermal transport theory: A review and a suggestion for future numerical model development, *Journal of Heat Transfer* 133 (1) (2011) 011011. doi:10.1115/1.4002362.
45. G. Pontrelli, F. de Monte, Mass diffusion through two-layer porous media: an application to the drug-eluting stent, *International Journal of Heat and Mass Transfer* 50 (17–18) (2007) 3658–3669. doi:10.1016/j.ijheatmasstransfer.2006.11.003.
46. M. A. Lovich, E. R. Edelman, Computational simulations of local vascular heparin deposition and distribution, *American Journal of Physiology—Heart and Circulatory Physiology* 271 (5) (1996) H2014–H2024. arXiv:<http://ajpheart.physiology.org/content/271/5/H2014>. full.pdf+html. URL <http://ajpheart.physiology.org/content/271/5/H2014.abstract>.
47. T. Seo, L. G. Schachter, A. I. Barakat, Computational study of fluid mechanical disturbance induced by endovascular stents, *Annals of Biomedical Engineering* 33 (2005) 444–456. doi:10.1007/s10439-005-2499-y.
48. F. Migliavacca, F. Gervaso, M. Prosi, P. Zunino, S. Minisini, L. Formaggia, G. Dubini, Expansion and drug elution model of a coronary stent, *Computer methods in biomechanics and biomedical engineering* 10 (1) (2007) 63–73.
49. G. Pontrelli, F. de Monte, A multi-layer porous wall model for coronary drug-eluting stents, *International Journal of Heat and Mass Transfer* 53 (19–20) (2010) 3629–3637. doi:10.1016/j.ijheatmasstransfer.2010.03.031.
50. V. B. Kolachalama, A. R. Tzafiriri, D. Y. Arifin, E. R. Edelman, Luminal flow patterns dictate arterial drug deposition in stent-based delivery, *Journal of Controlled Release* 133 (1) (2009) 24–30. doi:10.1016/j.jconrel.2008.09.075.
51. G. Vairo, M. Cioffi, R. Cottone, G. Dubini, F. Migliavacca, Drug release from coronary eluting stents: A multidomain approach, *Journal of Biomechanics* 43 (8) (2010) 1580–1589. doi:10.1016/j.jbiomech.2010.01.033.
52. V. V. Koulich, J. Lage, C. Hsia, R. Johnson, A porous medium model of alveolar gas diffusion, *Journal of Porous Media* 2 (3) (1999) 263–275.
53. V. V. Kulish, J. L. Lage, C. C. W. Hsia, J. Robert L. Johnson, Three-dimensional, unsteady simulation of alveolar respiration, *Journal of Biomechanical Engineering* 124 (5) (2002) 609–616. doi:10.1115/1.1504445.
54. M. A. Lewis, M. R. Owen, The mechanics of lung tissue under high-frequency ventilation, *SIAM Journal on Applied Mathematics* 61 (5) (2001) 1731–1761. doi:10.1137/S0036139999363652.
55. B. Lande, W. Mitzner, Analysis of lung parenchyma as a parametric porous medium, *Journal of Applied Physiology* 101 (3) (2006) 926–933. arXiv:<http://jap.physiology.org/content/101/3/926.full.pdf+html>, doi:10.1152/jappphysiol.01548.2005.
56. F. Kuwahara, Y. Sano, J. Liu, A. Nakayama, A porous media approach for bifurcating flow and mass transfer in a human lung, *Journal of Heat Transfer* 131 (10) (2009) 101013. doi:10.1115/1.3180699.
57. R. Cimrman, E. Rohan, On modelling the parallel diffusion flow in deforming porous media, *Mathematics and Computers in Simulation* 76 (1–3) (2007) 34–43, mathematical Modelling and Computational Methods in Applied Sciences and Engineering. doi:10.1016/j.matcom.2007.01.034.
58. Z. Liao, C. K. Poh, Z. Huang, P. A. Hardy, W. R. Clark, D. Gao, A numerical and experimental study of mass transfer in the artificial kidney, *Journal of Biomechanical Engineering* 125 (4) (2003) 472–480. doi:10.1115/1.1589776.
59. W. Ding, L. He, G. Zhao, H. Zhang, Z. Shu, D. Gao, Double porous media model for mass transfer of hemodialyzers, *International Journal of Heat and Mass Transfer* 47 (22) (2004) 4849–4855. doi:10.1016/j.ijheatmasstransfer.2004.04.017.
60. S. W. Smye, C. J. Evans, M. P. Robinson, B. D. Sleeman, Modelling the electrical properties of tissue as a porous medium, *Physics in Medicine and Biology* 52 (23) (2007) 7007. URL <http://stacks.iop.org/0031-9155/52/i=23/a=016>.
61. L. Dai, R. M. Miura, A lattice cellular automata model for ion diffusion in the brain-cell microenvironment and determination of tortuosity and volume fraction, *SIAM Journal on Applied Mathematics* 59 (6) (1999) pp. 2247–2273. URL <http://www.jstor.org/stable/118424>.
62. P. N. Sen, P. J. Basser, Modeling diffusion in white matter in the brain: A composite porous medium, *Magnetic Resonance Imaging* 23 (2) (2005) 215–220, proceedings of the Seventh International Conference on Recent Advances in MR Applications to Porous Media. doi:10.1016/j.mri.2004.11.014.
63. A. Wagner, W. Ehlers, A porous media model to describe the behaviour of brain tissue, *PAMM* 8 (1) (2008) 10201–10202. doi:10.1002/pamm.200810201.
64. P. Drysdale, J. Huber, P. Robinson, K. Aquino, Spatiotemporal bold dynamics from a poroelastic hemodynamic model, *Journal of Theoretical Biology* 265 (4) (2010) 524–534. doi:10.1016/j.jtbi.2010.05.026.
65. E. Elshehawey, N. Eldabea, E. Elghazya, A. Ebaid, Peristaltic transport in an asymmetric channel through a porous medium, *Applied Mathematics and Computation* 182 (1) (2006) 140–150. doi:10.1016/j.amc.2006.03.040.
66. S. Maiti, J. Misra, Peristaltic flow of a fluid in a porous channel: A study having relevance to flow of bile within ducts in a pathological state, *International Journal of Engineering Science In Press*, Corrected Proof. doi:10.1016/j.ijengsci.2011.05.006.
67. D. Tripathi, S. Pandey, S. Das, Peristaltic transport of a generalized burg-ers' fluid: Application to the movement of chyme in small intestine, *Acta Astronautica* 69 (1–2) (2011) 30–38. doi:10.1016/j.actaastro.2010.12.010.
68. M. Kothandapani, S. Srinivas, Non-linear peristaltic transport of a newtonian fluid in an inclined asymmetric channel through a porous medium, *Physics Letters A* 372 (8) (2008) 1265–1276. doi:10.1016/j.physleta.2007.09.040.

69. V. Rathod, M. Channakote, A study of ureteral peristalsis in cylindrical tube through porous medium, *Advances in Applied Science Research* 2 (3) (2011) 134–140.
70. Y. Sim, C. V. Chrysikopoulos, Virus transport in unsaturated porous media, *Water Resources Research* 36 (1) (2000) 173–179. URL <http://gram.eng.uci.edu/~costas/pdffiles/A32.pdf>.
71. J. F. Schijven, J. Simunek, Kinetic modeling of virus transport at the field scale, *Journal of Contaminant Hydrology* 55 (1–2) (2002) 113–135. doi:10.1016/S0169-7722(01)00188-7.
72. G. R. Barth, M. C. Hill, Parameter and observation importance in modelling virus transport in saturated porous media—investigations in a homogenous system, *Journal of Contaminant Hydrology* 80 (3–4) (2005) 107–129. doi:10.1016/j.jconhyd.2005.06.012.
73. P. M. Oates, C. Castenson, C. F. Harvey, M. Polz, P. Culligan, Illuminating reactive microbial transport in saturated porous media: Demonstration of a visualization method and conceptual transport model, *Journal of Contaminant Hydrology* 77 (4) (2005) 233–245. doi:10.1016/j.jconhyd.2004.12.005.
74. N. Tufenkji, Modeling microbial transport in porous media: Traditional approaches and recent developments, *Advances in Water Resources* 30 (6–7) (2007) 1455–1469, biological processes in porous media: From the pore scale to the field. doi:10.1016/j.advwatres.2006.05.014.
75. S. Bhattacharjee, J. N. Ryan, M. Elimelech, Virus transport in physiologically and geochemically heterogenous subsurface porous media, *Journal of Contaminant Hydrology* 57 (2002) 161–187. URL <http://gram.eng.uci.edu/~costas/pdffiles/A32.pdf>.
76. H. M. Bekhit, M. A. El-Kordy, A. E. Hassan, Contaminant transport in groundwater in the presence of colloids and bacteria: Model development and verification, *Journal of Contaminant Hydrology* 108 (3–4) (2009) 152–167. doi:10.1016/j.jconhyd.2009.07.003.
77. P. K. Sharma, R. Srivastava, Numerical analysis of virus transport through heterogeneous porous media, *Journal of Hydro-environment Research* 5 (2) (2011) 93–99. doi:10.1016/j.jher.2011.01.001.
78. Y. Zhang, Generalized dual-phase lag bioheat equations based on nonequilibrium heat transfer in living biological tissues, *International Journal of Heat and Mass Transfer* 52 (21–22) (2009) 4829–4834. doi:10.1016/j.ijheatmasstransfer.2009.06.007.
79. M. M. Chen, K. R. Holmes, Microvascular contributions in tissue heat transfer, *Annals of the New York Academy of Sciences* 335 (1) (1980) 137–150. doi:10.1111/j.1749-6632.1980.tb50742.x.
80. H. H. Pennes, Analysis of tissue and arterial blood temperature in the resting human forearm, *J. Appl. Physiol.* 1 (2) (1948) 93–122.
81. A. Nakayama, F. Kuwahara, A general bioheat transfer model based on the theory of porous media, *International Journal of Heat and Mass Transfer* 51 (11–12) (2008) 3190–3199. doi:10.1016/j.ijheatmasstransfer.2007.05.030.
82. D. Nield, A. Kuznetsov, A bioheat transfer model: Forced convection in a channel occupied by a porous medium with counterflow, *International Journal of Heat and Mass Transfer* 51 (23–24) (2008) 5534–5541, biomedical-Related Special Issue. doi:10.1016/j.ijheatmasstransfer.2008.04.015.
83. A. Belmiloudi, Parameter identification problems and analysis of the impact of porous media in biofluid heat transfer in biological tissues during thermal therapy, *Nonlinear Analysis: Real World Applications* 11 (3) (2010) 1345–1363. doi:10.1016/j.nonrwa.2009.02.025.
84. K. Mitra, S. Kumar, A. Vedavaz, M. Moallemi, Experimental evidence of hyperbolic heat conduction in processed meat, *Journal of Heat Transfer* 117 (1995) 568–573.
85. C. Cattaneo, A form of heat conduction equation which eliminates the paradox of instantaneous propagation, *Comp. Rend.* 246 (1958) 431–433.
86. A. Narasimhan, S. Sadasivam, Non-fourier bio heat transfer modeling of retinal laser surgery, *Physical Review E Under Review*.
87. A. Narasimhan, K. K. Jha, L. Gopal, Transient simulations of heat transfer in human eye undergoing laser surgery, *International Journal of Heat and Mass Transfer*. 53 (2011) 482–490. doi:10.1016/j.ijheatmasstransfer.2009.09.007.
88. H.-S. Kou, T.-C. Shih, W.-L. Lin, Effect of the directional blood flow on thermal dose distribution during thermal therapy: an application of a green's function based on the porous model, *Physics in Medicine and Biology* 48 (11) (2003) 1577. URL <http://stacks.iop.org/0031-9155/48/i=11/a=307>.
89. Y. He, H. Liu, R. Himeno, J. Sunaga, N. Kakusho, H. Yokota, Finite element analysis of blood flow and heat transfer in an image-based human finger, *Computers in Biology and Medicine* 38 (5) (2008) 555–562. doi: 10.1016/j.combiomed.2008.02.002.
90. P. Yuan, Numerical analysis of an equivalent heat transfer coefficient in a porous model for simulating a biological tissue in a hyperthermia therapy, *International Journal of Heat and Mass Transfer* 52 (7–8) (2009) 1734–1740. doi:10.1016/j.ijheatmasstransfer.2008.09.033.
91. S. Mahjoob, K. Vafai, Analytical characterization of heat transport through biological media incorporating hyperthermia treatment, *International Journal of Heat and Mass Transfer* 52 (5–6) (2009) 1608–1618. doi:10.1016/j.ijheatmasstransfer.2008.07.038.
92. H.-X. Zhou, Q&a: What is biophysics?, *BMC Biology* 9 (1) (2011) 13. doi:10.1186/1741-7007-9-13.
93. W. Gratzer, Biophysics—whence, whither, wherefore—or hold that hyphen, *BMC Biology* 9 (1) (2011) 12. doi:10.1186/1741-7007-9-12.



Arunn Narasimhan is an Associate Professor in the Department of Mechanical Engineering at the Indian Institute of Technology Madras, Chennai, India. He received his Ph.D. degree from the Mechanical Engineering Department of the Southern Methodist University in 2002. He has also worked as a staff research engineer in the Microlithography Division of FSI International, Allen, Texas, USA. His primary research interest for the past ten years has been in modelling hydrodynamics and heat transport in porous media. Heat transfer and fluid flow in biological systems is his current research interest.